Liquid crystalline metal phthalocyanines: Structural organization on the substrate surface

BASOVA, Tamara, HASSAN, Aseel <http://orcid.org/0000-0002-7891-8087>, DURMUŞ, Mahmut, GÜREK, Ayse Gül and AHSEN, Vefa

Published version

BASOVA, Tamara, HASSAN, Aseel, DURMUŞ, Mahmut, GÜREK, Ayse Gül and AHSEN, Vefa (2016). Liquid crystalline metal phthalocyanines: Structural organization on the substrate surface. Coordination Chemistry Reviews, 310, 131-153.

Liquid crystalline metal phthalocyanines: structural organization on the substrate surface

Tamara Basova,[1,2*] Aseel Hassan,[3] Mahmut Durmuş,[4] Ayse Gül Gürek,[4] Vefa Ahsen[4]

[1]Nikolaev Institute of Inorganic Chemistry SB RAS, 3 Lavrentiev Ave., Novosibirsk, Russia
[2]Novosibirsk State University, Pirogova Str. 2, Novosibirsk, Russia
[3]Materials and Engineering Research Institute, Sheffield Hallam University, Sheffield S1 1WB, UK [4]Gebze Technical University, Department of Chemistry, Gebze, Kocaeli, Turkey

Abstract

The use of metallo phthalocyanines (MPcs) in technological applications requires certain methodological approaches for thin film fabrication. Among these applications is the implementation of MPc films in electronic devices such as organic field-effect transistors (OFETs) and photovoltaic (PV) devices. For such applications the control of alignment and ordering of MPc molecules within the films remains a considerable challenge. This review provides an overview of films' growth of mesogenic MPcs offering systematic analysis of the influence of different factors on the structural organization of liquid crystalline phthalocyanine films, including phthalocyanines molecular structure, regimes of heating, substrate materials, and type of interfaces. The achievements in the development of methods and approaches for the formation of liquid crystalline phthalocyanine films with controllable alignment and ordering are discussed in sufficient details.

Keywords: metal phthalocyanines; liquid crystals; thin films; film alignment

* Corresponding author: Nikolaev Institute of Inorganic Chemistry SB RAS, 3 Lavrentiev Ave., Novosibirsk, 630090 Russia, basova@niic.nsc.ru, tel. +73833302814

Content

1. Introduction

The unique physicochemical properties of phthalocyanines and their metal complexes (MPcs) have made them subjects of numerous fundamental and applied studies. The ability to tailor their chemical structure allows their semiconducting properties to be modified to suit a broad range of technological applications. This can be controlled through the synthesis process of the MPcs altering parameters such as central metal atoms, peripheral substituents and conjugated structure [1]. In dependence on molecular structure, MPcs can be volatile or unvolatile in vacuum, soluble or insoluble in organic solvents and in water [2]. They can form liquid crystalline phases [3, 4], different linear, net and 3D polymeric structures [5]. The choice of thin films deposition method is dependent on MPc molecular properties [6].

Methods like vacuum evaporation, spin coating and Langmuir-Blodgett (LB) technique have been extensively used to produce thin films of MPcs. The morphology and structure of the MPc films have strong bearing on their electrical and optical properties as well as on the films' sensing characteristics. Therefore in order to optimize the properties of the films for one or another technological application it is crucially important to produce films with sufficient level of uniformity as well as controllable architecture and molecular ordering.

Self alignment of MPc molecules into columnar molecular stacks is the consequence of the strong overlap between the π-orbitals of adjacent molecules. This alignment results in the formation of one-dimensional wires which are surrounded by an insulating sheet that are produced by the aliphatic chains. Such films with ordered columnar structure demonstrate anisotropic properties including a highly anisotropic charge carrier mobility. The latter is an electronic feature which is found of crucial importance in electronic device applications. Metal phthalocyanines have wide application as active layers in various electronic devices such as organic solar cells [7, 8], organic light-emitting diodes (OLED) [9-11], organic field effect transistors (OFET) [12, 13], chemical sensors [14, 15] as well as several other applications. For all these applications, ordered structures and smooth surfaces of the MPc films play significant role in achieving devices with significantly improved performance.

Organization of monolayers and ultrathin films of porphyrin and phthalocyanine derivatives on surfaces has been extensively discussed in several reviews [16-18]. These reviews describe a number of approaches which are implemented in order to achieve nanoscale architectures on different substrates. Among these approaches are sublimation under ultrahigh vacuum conditions, immersion of surfaces into solutions to form adlayers as well as the deposition of solutions directly onto substrates in order to directly investigate the liquid–solid interface properties.

In general deposition of materials from solution followed by thermal annealing is a remarkably more simple and inexpensive method in comparison with vacuum-processing techniques for the manufacturing of organic electronic devices [6]. Film deposition of phthalocyanine compounds by Langmuir-Blodgett (LB) method is a very useful approach, however this method imposes many restrictions and requirements to the molecular structure. Some aspects of the effect of different parameters on the orientation of MPc molecules at the air-water interface and in the LB thin layers are discussed in the literature [19].

Since the pioneering work in 1982 by Piechocki and co-authors [20], mesogenic phthalocyanines have attracted significant attention due to their intriguing optical and electronic properties making them attractive in optoelectronic device applications. These materials are able to self-organize into mesophases possessed order and mobility. Being an intermediate state between the crystal and the isotropic liquid, the macroscopic behavior of these mesophases is determined by the molecular structure and properties. Disc-like phthalocyanines stack as columnar structures, leading to the formation of 1D conductors along the columns axis. This is the result of the efficient overlap of the π-orbitals in adjacent macrocycles, whereas the surrounding long alkyl chains play the role of a laterally isolating shield [21-23]. Within this type of structure the molecules are arranged in stacks on top of one another forming columns of molecules which assume a regular 2D lattice which are predominantly classified in terms of their symmetry. In a similar fashion as the smectic counterparts, these columnar structures exhibit a rich poly-mesomorphism. Columns packed as a regular hexagonal lattice are called Col_h and on a rectangular lattice, Col_r; an oblique lattice packing is called Col_{ob}, and so on. (Fig. 1).

Figure 1

Columnar liquid crystals (LC) exhibit large charge carrier mobilities as well as large exciton diffusion lengths along the columnar stacks axis; these are essential electronic characteristics that make these materials of significant importance in organic electronic applications [21, 24-28]. As pointed out earlier such characteristics are the result of π-orbitals overlapping between adjacent discotic molecules within the columns, providing 1D charge transport pathway. When layers of these columnar liquid crystalline molecules are aligned between two metal electrodes they can form active layers in organic optoelectronic devices. The latter is a relatively new field of research where the unique properties of this class of materials play critical role in the development of simple, low cost and mechanically flexible device fabrication route. Discotic liquid crystals however are already in use as active layers of some electronic devices as OFET, light-emitting devices, photovoltaic cells and electronic nose.

A key issue for discotic LCs is the alignment of their disc-like molecules which self-assemble into columnar aggregates and exhibit one-dimensional charge transport along the columnar axes [29]. The columnar axes should be oriented perpendicular to the metal electrodes for efficient charge injection and collection. In photovoltaic applications [13, 30] the homeotropic alignment of the molecular columns, that facilitate the current flows between the top and bottom electrodes, is required (Fig. 2a). On the other hand, planar or homogeneous alignment, where the columnar axes are oriented parallel to the substrate surface, should be achieved, for device applications as in field effect transistors (Fig. 2b).

Figure 2

The molecular design of discotic liquid crystals, as well as their structure-property relationship, have been the subject of several reviews [21, 31, 32]. A review article written by S. Kumar [32] was devoted to chemical aspects of the formation of supramolecular assemblies of discotic molecules with more emphasis placed on basic design principles and synthesis of some frequently used discotic liquid crystals (DLC), while the problems of structural organization of DLC films on substrate surfaces were not discussed. Another critical review published by Geerts *et al.* in 2007 [21] covers aspects associated with molecular design, supramolecular structure and deposition of ordered films of DLCs. However most published data in this field are devoted to hexabenzocoronene, triphenylene derivatives as well as polycyclic aromatic hydrocarbons. Very limited examples of mesogenic phthalocyanine derivatives are also described, however a range of questions concerning the influence of the phthalocyanine molecular structure and the substituents type on the films alignment were not sufficiently answered. It is also worthwhile mentioning that the number of published work (about 50 references) on the investigation of the alignment of mesogenic MPc films have been published after 2007. In a mini review written by Martínez-Díaz and Bottari [33] a brief overview was provided describing the work of Spanish researchers in preparing organized phthalocyanine-based supramolecular systems. In a more recent review [31] Fleischmann *et al* have summarized state of the art applications of different classes of DLCs in some electronic devices.

In this review an overview of the growth behavior of thin films of mesogenic metal phthalocyanines is provided. After illustrating the liquid-crystalline properties of the substituted phthalocyanines used for films' deposition main emphasis is placed on the systematic analysis of the influence of different factors on the structural organization of liquid crystalline phthalocyanine thin films, including phthalocyanines molecular structure, regimes of heating, substrate materials, and type of interfaces. The achievements in the development of methods and

approaches for the formation of liquid crystalline phthalocyanine films with controllable alignment and ordering are discussed in sufficient details.

2. Phthalocyanines with liquid crystalline properties

Since 1982 when Piechocki and co-workers [20] synthesized the first mesogenic phthalocyanines the mesophase structure of a significant number of substituted phthalocyanines and porphyrins were investigated [34]. These include phthalocyanines with eight linear alkyl [35], alkoxymethyl [36, 37] and alkoxy [37-39] substituents which demonstrated transitions from the crystalline phases to the mesophases at elevated temperatures. Various MPcs with different substituents were synthesized, however, structure and properties of thin film of a small number of these LC phthalocyanines were reported. According to diffuse diffraction features in XRD patterns the transformation of the crystalline phase to the LC phase at elevated temperature was accompanied by the melting of the long alkyl and alkoxy substituents [38]. In condensed phase the molecules are often arranged in herringbone or tilted structure as those commonly seen in acene crystals. This is essentially caused by the interaction between the aromatic cores of the molecules whereas a cofacial arrangement is favored due to the influence arising from the aliphatic side chains on the packing energy. The phase behavior is mainly explained by the interplay of these energies; this is further established by the fact that the melting of the long alkyl substituents accompanies the change from a tilted packing to a cofacial one [40].

In general, the use of phthalocyanine compounds in technical applications can mainly be envisaged through producing them as thin films. It is therefore critically important to understand the columnar arrangement of metal pthalocyanine molecules within the solid films' at different scales ranging from the diameter of an individual column to the size of some micrometers.

In this review the LC properties of the substituted phthalocyanines used for film deposition are considered.

One of the main advantages of tetra-substituted LC MPcs over their octa-substituted counterparts is that they can usually be obtained as a mixture of the four regioisomers formed during the cyclotetramerization reaction [41-42]. The occurrence of the mixture decreases the temperatures of the phase transition in comparison with the octa-substituted analogues. Furthermore, crystallization of the LC MPc is prevented due to the occurrence of the four isomers [40]. Likewise, the presence of branched side chains around the Pc ring has the advantage of preventing crystallization due to the presence of an asymmetric carbon atom in each alkyl substituent which creates a large number of diastereoisomers. Another advantage stems out from this branching which makes the substituents more bulky and thus destabilizes their packing by steric hindrance and thus decreasing the temperature of transition from LC to

isotropic liquid. The introduction of laterally branched alkyl chains (2-octyldodecyloxy and 2-decyltetradecyloxy**) (1a, 1b** in Table 1**)** leads to that the compound forms liquid crystalline phase at room temperature.

Table 1

Analysis of thermal data obtained for 2(3),9(10),16(17),23(24)-tetra-2-octyldodecyloxy and (2-decyltetradecyloxy) phthalocyanines (**1a, 1b)** has been summarized in Table 2. **1a, 1b** derivatives exhibit a transition between a columnar hexagonal (Col_h) and a columnar rectangular (Col_r) phase [43]. For compounds **1a** and **1b**, a low-temperature transition occurs at 68 and 60 °C, respectively. No crystalline phase has been detected in the range from room temperature up to 230 ^oC [44]. At small angles the high-temperature mesophases of compounds **1a, 1b** exhibit reflections in XRD pattern, associated with reciprocal spacing that follows the ratio 1:√3:√4:√7 which are indexed as 10, 11, 20, and 21 of the 2D hexagonal lattices. A halo between 4.6 and 5.1 Å was observed in the wide-angle region which is related to the average distance of the liquid like alkyl substituents. The diffraction patterns of **1a** and **1b** below 68 and 60 °C, respectively, are consistent with Col_r mesophase. The intercolumnar distances of the high-temperature Col_h and low-temperature Col_r mesophases are only slightly different, as deduced from their cell parameters. Furthermore, a pseudo focal-conic texture is observed below 226 and 180 °C for **1a** and **1b,** respectively, typical of columnar hexagonal mesophases (Col_h), when they were subjected to fast cooling from isotropic melt [45]. The optical texture develops to a “fingerprint” texture at lower temperatures which is a characteristic of columnar rectangular mesophases (Col_r) [46]. A Col_r mesophase with regularly aligned columns, obtained upon cooling from a homeotropically aligned Col_h mesophase, was first reported by Tant and co-workers [43].

Table 2

A rigid disc-like aromatic core as well as several flexible long alkoxy or alkyl chains as peripheral substituents are essential to exhibit LC properties. However phthalocyanine derivative (**2**) substituted by four monoazacrown ether groups instead of long alkyl chains (Fig. 3a) exhibits LC transition [47].

Figure 3

In 1987 it was demonstrated for the first time that 15-crown-5 substituted MPc shows a Col_{tet} mesophase [48]. The flexible crown macrocycles play a similar role as the long alkyl chains in

providing LC properties. Several aza-crown ether-substituted phthalocyanines have been studied [49-52]. To improve the LC properties, solubility, as well as the amphiphilic character of the compounds various substituents have been attached through the nitrogen atoms of the aza-crown moieties. The Differential Scanning Calorimetry (DSC) measurement of **2** shows a broad peak at ~100 ^{o}C for the heating cycle (ΔH = 12.64 kJ/mol) and at ~90 ^{o}C (ΔH = 13.30 kJ/mol) for the cooling cycle. Decomposition temperature of the CuPc **2** is about 325-400 ^{o}C (determined by Thermal Gravimetric Analysis, TGA). Analysis of the DSC measurements indicates that **2** exhibits a thermotropic LC behaviour above 97 ^{o}C. The Cu(II) phthalocyanine derivative has a hexagonal columnar structure. Good mosaic texture of CuPc **2** mesophase was obtained by slow cooling, at the rate of 5 ^{o}C min^{-1}, from the isotropic melt. Phase transition of compound **2** from mesophase to isotropic liquid takes place at the temperature of 322 ^{o}C. Fig. 4a presents the texture of this compound observed under crossed polarizers at 130 ^{o}C [47].

Figure 4

In other work, LC M(II)Pc (M= Zn, Ni, Cu) (**3-5**) derivatives having monoazacrown ether moieties with long alkyloxyphenyl N-pivotal groups have been synthesized [52] (Fig. 3b). These derivatives show Col_h mesophases over a wide temperature range [53]. DSC investigations indicate that compounds NiPc(**3**), and CuPc(**5**) demonstrate a thermotropic LC behavior above 60 °C and 73 °C, respectively. ZnPc derivative on the other hand exhibits a thermotropic LC behavior even at room temperature (Table 3).

Table 3

The polarizing optical microscopy data shows that the compounds **3-5** exhibit very similar textures to those reported in the literature for other columnar mesophases [54, 55]. On slow cooling from 300 °C at the rate of 5 °C min^{-1}, a good texture of phthalocyanines mesophase was obtained. A polarizing optical microscopy texture of CuPc derivative at 180 °C is shown in Fig. 4b.

Six octakis(dialkoxyphenoxy)phthalocyaninatocopper(II) complexes (**6a-f**) (abbreviated as $[(C_nO)_2PhO]_8PcCu$ (n=9-14)) have been synthesized by Ohta *et al* [56] (Table 4). **6a-f** derivatives form several mesophases: Col_h, Col_{r1}, Col_{r2}, Col_{r3}, Col_{tet} and Cub phases. The cubic mesophase, Cub, has been obtained for the first time in the case of LC phthalocyanines.

Table 4

Fig. 5 shows the dependence of phase transition temperatures on the number of carbon atoms in the alkoxy chain (n).

Figure 5

Most discotic LCs show columnar mesophases. Octa-alkoxy peripherally-substituted phthalocyanine molecules stack one above another to form columns. These columns are ordered in a hexagonal two-dimensional lattice, which therefore form a hexagonal columnar mesophases (Col_h). Table 4 shows 2,3,9,10,16,17,23,24-octakis(alkoxy) substituted phthalocyanine derivatives (MPc-OC_n) with various central metal ions as well as with various peripheral chains. Compounds **7a-e**, **8a-e**, **9a-e** (Table 4) are characterised with high thermal stability and therefore the temperature range of the existence of their mesophases extends over 250 °C. The high stability of these molecules is ascribed both to the strong van der Waals interactions between the alkyl substituents and to the π-π interactions between the MPc aromatic cores.

The occurrence of a two-dimensional hexagonal lattice was confirmed with high temperature XRD measurements. The melting point increases in the order $Ni^{II} < Cu^{II} \approx Co^{II} < Zn^{II}$ independent of the chain length and are higher than that of the metal-free analogue. Only compounds with long alkyl chains ($C_{16}H_{33}O$) (**9a-e**) exhibit clearing points, whereas the other compounds start to decompose before reaching this point. The clearing point did not show dependence on the type of the central metal ion [57, 58]. 2,3,9,10,16,17,23,24-octakis(octyloxy)-29H,31H-phthalocyanine (H_2Pc-OC_8) (**7e**) totally devoids of polymorphism and forms only Col_{ho} mesophase.

LC properties of MPcs can be varied by the introducing alkyl or alkoxy chains at the peripheral and non-peripheral positions of Pc macrocycle [59]. Sterically hindered peripheral ((2,9(10),16(17),23(24)-positions)-tetra(13,17-dioxanonacosane-15-hydroxy)-substituted phthalocyanines (**10a-c**) (Table 1) exhibit liquid crystalline properties at room temperature [60] whereas analogous non-peripheral derivatives are liquids at room temperature. Table 5 presents a summary of phase transition temperatures and enthalpy changes of **10a-c** derivatives.

Table 5

Fig. 6 shows polarizing optical microscopy images of compounds **10a-c** recorded at room temperature. Powder diffraction patterns of the three derivatives comprise the reflections typical for the ordered Col_h mesophase; obtained XRD data of these compounds are summarized in Table 6 [60].

Figure 6

Table 6

The electronic effect of the linking group can be rationalized by simple theory of Hunter and Sanders [61] for electrostatic interactions of aromatic compounds. This theory suggests that the attractive interaction between adjacent aromatic molecules originates from the attraction between the negatively charged π-system and positively charged σ-bond skeleton. The extremely large range of most MPc mesogens indicates that π-π interactions, in addition to disc-shaped anisotropy, play an important role in helping to stabilize columnar mesophases. Therefore, MPcs containing electron-withdrawing linking groups should display columnar mesophases with enhanced thermal stability [40].

The synthesis of long alkylthio substituted derivatives is much easier than the synthesis of MPcs substituted with alkyl chains. The first octasubstituted MPc derivative with long alkylthio chains (Table 4) was synthesized in 1991 [62]. The electron donation capacity of the substituents decreases in the order of OR>$ROCH_2$>R>RS. As a result of the zero Hammett σ value, the alkylthio group is neither electron donating nor electron withdrawing. This type of substituent however becomes an electron-withdrawing group when it is oxidized to alkylsulfanyl group. A LC triphenylene derivative substituted by alkylthio groups exhibits charge carrier mobility in its discotic mesophase that is much larger than that observed for conventional organic semiconductors [63]. This example demonstrates the effect of sulfur atoms on the mesophase conductivity. The first examples of columnar mesomorphism of octakis(octylthio)-substituted phthalocyanine and its Zn(II) and Cu(II) complexes have been reported by Eichhorn and Wöhrle [64]; all derivatives have shown a Col_h mesophase over a broad range of temperatures. Monomer and dimer stacking co-exists in the Col_h mesophases, however, the parallel dimer stacking gradually changes into herringbone dimer stacking by the effect of heating (thermal fluctuation). More ordered stacking within the columns occurs in the mesophase of copper complexes as compared to the mesophases of the H_2Pc derivative [65].

The synthesis of octakis-hexyl and dodecyl-thio-substituted NiPc (**11a,12a**) and CuPc (**11b,12b**) derivatives demonstrating thermotropic phase behavior has been carried out by Gürek *et al* [66]. As can be seen from Table 7, both nickel (II) (**11a**, **12a**) and copper (II) (**11b**) phthalocyanine derivatives show only one mesophase, Col_h. Typical columnar mesophase textures were observed using polarizing optical microscopy which show large cylindrical domains as well as large homeotropic areas. A mosaic texture for $(C_6S)_8$PcCu (**11b**), typical for Col_h mesophase, is presented in Fig. 7a. The phthalocyanine derivatives **11a**, **12a**, and **11b** are

liquid crystalline over a wide temperature range up to 300 °C. The substitution with alkylthio groups in compounds **11a** and **12a** results in decreasing the temperature of transition to LC phase and therefore in broadening the mesophase range in comparison to the oxygen containing counterparts [38, 39].

Table 7

Figure 7

Fig. 7b shows XRD pattern of $(C_6S)_8PcCu$ (**11b**) as an example. XRD patterns of compounds **11a**, **12a**, and **11b** reveal the reflections with reciprocal spacings values of 1:√3:√4:√7:√9. These spacings are typical of a discotic hexagonal columnar (Col_h) mesophase [67, 68].

Mesomorphic lead phthalocyanines (PbPc) offer an intriguing and very promising class of compounds. The first nesomorphic PbPc was synthesised in 1987 [36, 69]. Alkoxymethyl substituted phthalocyaninato lead(II) complexes ($PbPcR_8$, R= $-CH_2OC_nH_{2n+1}$; n= 8, 12) gave a stable Col_h mesophase even at room temperature. This analogue however sterically destabilizes the cofacial columnar structure when compared to other MPc mesogens, and significantly decreases both melting and clearing points [40]. Furthermore, the type of mesophase as well as the transition temperature determine by the nature of the linking atom between alkyl chains and aromatic core of these mesogens [70, 71]. Research interest has also been focused on alkylthio-substituted PbPc derivatives, mostly due to the improved conductivity compared to their alkyl and alkoxy analogues. Octakis and tetrakis (alkylthio)-substituted LC PbPcs [**13a, b** (Table 4) and **14** (Table 1)] have been synthesized and described in the literature [72, 73].

Table 8

Table 8 provides summary of data related to phase of these PbPc derivatives. Using DSC measurements, the liquid crystalline phase and the isotropic phase transition temperatures are determined from the two prominent peaks observed in the DSC curves for both **13a,b** and **14**. The photomicrographs of the mesophase of **13a** and **13b** are shown in Fig. 8. A fan-shaped texture typical of Col_h mesophases were observed for both phthalocyanines. A decrease in the temperatures of phase transition from mesophase to isotropic liquid was observed for **13a** and **13b** compared to the metal-free and Cu(II) analogues [65]. The clearing point of **14** is lower than that of **13a,b** due to the fact that **14** is a mixture of four isomers.

Figure 8

Microscopic observations as well as XRD measurements were used to identify the mesophases for compounds **13a,b** and **14**; XRD reflections typical of a columnar mesophases of substituted Pcs were observed in the powder diffraction patterns of the three derivatives [72, 73].

In another work [74], the synthesis of tetrakis octylthio- and octyl-oxysubstituted PbPcs (**15-18**) with the substituents both in peripheral (Table 1) and nonperipheral (Table 9) positions has been described. Phase transition temperatures of these PbPc derivatives are presented in Table 10. Peripherally alkoxy substituted PbPc derivative (**17**) (Table 10) does not form any mesophase and melts at 63 °C. X-ray phase analysis has verified the formation of Col_h mesophase for the peripherally substituted derivatives (**15**, **16**) (Table 1) whereas the nonperipherally alkoxy substituted derivative (**18**) exhibited a columnar tetragonal (Col_{tet}) mesophase. The cofacial columnar structure is sterically destabilized because of big Pb atoms lying outside the plane of phthalocyanine macrocycle. This is also believed to cause a significant reduction in both melting and clearing points. Furthermore, nonperipherally substituted derivatives have lower clearing points in comparison with their peripherally substituted analogues.

Table 9

Table 10

The birefringence textures of thin films of **15, 16,** and **18** deposited between two glass substrates were observed during a very slow cooling of the samples from isotropic melts; photomicrographs of the mesophases of these derivatives are displayed in Fig. 9.

Figure 9

Ohta and co-workers have obtained a series of bis[octakis-(alkylthio)phthalocyaninato] rare-earth metal(III) complexes $[(C_nS)_8Pc]_2M$ (where M is Eu(III), Tb(III), and Lu(III); n = 8, 10, 12, 14, and 16), and their mesomorphism was studied in sufficient details [75]. In other works [76, 77], the hexylthiosubstituted rare-earth metal bisphthalocyanines {$[(C_6S)_8Pc]_2Lu$ (**19**), $[(C_6S)_8Pc]_2Gd$ (**20**), $[(C_6S)_8Pc]_2Dy$ (**21**), and $[(C_6S)_8Pc]_2Sm$ (**22**)} were synthesized and characterized (Fig. 10).

Figure 10

These complexes assume similar mesogenic properties as those demonstrated by other alkylthio-substituted bisphthalocyanines. Also, the bisphthalocyanines substituted with hexylthio groups $[(C_6S)_8Pc]_2M$ (M= Lu (III), Gd(III), Dy(III), and Sm(III)) (**19-22**) have been obtained as single crystals. The data characterizing the phase transitions of the $[(C_6S)_8Pc]_2M$ (M= Lu(III), Gd(III), Dy(III), and Sm(III)) complexes (**19-22**) have been summarized in Table 11. The virgin state K_{1V} of $[(C_6S)_8Pc]_2Lu$ complex (**19**) transforms to K_{2V} crystalline phase at 102 °C when it was subjected to heat-treatment starting from room temperature. Further heating leads to transformation of the K_{2V} crystalline phase into a Col_h mesophase at 120 °C [77, 78].

Table 11

$[(C_6S)_8Pc]_2M$ (M= Gd(III), Dy(III), and Sm(III)) (**20-22**, respectively) complexes show only one mesophase, which is the Col_h. Octakis(alkylthio)-substituted monophthalocyanines are generally characterized with transition temperatures lower than those of their oxygen analogues [39]; these transition temperatures also decrease with increasing the chain length [38, 65]. Furthermore, the alkylthio substitution results in decreasing the melting point in octakis(alkylthio)-substituted bisphthalocyanines [75, 79, 80] in comparison with the analogue alkoxy-substituted derivatives $[(C_6O)_8Pc]_2Gd$, $[(C_6O)_8Pc]_2Dy$, and $[(C_6O)_8Pc]_2Sm$ [54, 81, 82].

Figure 11

Observation of clear birefringent textures using polarizing optical microscopy can be made upon cooling the samples from their melt. A POM image of the mesophase of Sm(III) derivative at 140 °C is shown in Fig. 11. This mesophase is the Col_h phase as determined by the typical fan-shaped texture which is usually observed for Col_h phases [77].

Compared to those of straight-chained analogues increasing the steric bulk of side-chains with short methyl or ethyl branches will result in phthalocyanine derivatives that possess mesophases with reduced thermal range and order. Members of the series MPc-*op*-OC_n containing branched side-chains will therefore tend to give the Col_{hd} [83] or even the rare non-columnar discotic nematic (N_d) mesophase [84], rather than the Col_{ho} mesophase encountered for straight-chained Pcs of this series.

Thioether substituents in phthalocyanine rings are effective in changing the MPc properties [62, 66, 85]. To determine the influence of the linking S atoms on the LC properties, sterically hindered and branched octa (13,17-dioxa nonacosane-15-sulfanyl)-substituted Ni(II) phthalocyanine (**23**) has been synthesized (Table 4) [86]. **23** shows a discotic mesophase properties over a significant temperature range including room temperature. The DSC measurements indicate that the compound forms only one mesophase and transforms to isotropic

liquid at 38 °C [86]. Compound **23** exhibits a spherulite-like liquid crystalline texture when cooled down at a rate of 5 °C min^{-1} from isotropic phase, and the sample is stored at room temperature for one day (Fig. 12).

Figure 12

The octa-substituted compound **23** exhibits seven Bragg reflections, which cannot be ascribed to a hexagonal lattice (Table 12). The XRD data can be indexed with a 2D rectangular lattice similar to other discotic LCs reported in the literature [87]. In the powder X-ray data of **23**, the two-dimensional unit cell is obtained with the a- and b-dimensions shown in Table 12. The appearance of two diffuse halos at about 4.8 and 4.2 Å suggests that the mesophase belongs to the Col_{rd}-type.

Table 12

Table 1 illustrates Ni(II) phthalocyanine derivative (**24**) substituted by four sterically hindered thia-bridged poly(oxyethylene) groups at pheripheral positions [88]. As it can be seen from Table 13, **24** shows only one mesophase, Col_h.

Table 13

Excellent fan-like texture of **24** (Fig. 13) have been obtained by slow cooling from its isotropic melt.

Figure 13

Summary of the obtained XRD data are presented in Table 14. Compound **24** exhibits reflections which are typical of a columnar mesophase of substituted MPcs as determined from its powder X-ray diffraction patterns [88]. The diffuse reflection at 4.35 Å observed for this compound indicates a lack of long-range translational order of the molecules within the stacks; this was attributed to the discotic hexagonal disordered Col_{hd} mesophase.

Table 14

Electronic, rather than steric, factors appear to be very influential in determining the thermal behavior of non-peripherally substituted Pcs. Interaction between non-peripheral substituent chains that are positioned on the neighboring benzo-moieties is the strongest steric interaction for

this type of side-chains, and it is the most likely reason for the displacement of some alkyl chains from the plane of the phthalocyanine macrocycle.

1,4,8,11,15,18,22,25-octaoctylphthalocyanine (**25)** has been synthesized by Cook *et al* (Table 15) [89, 90]. This compound demonstrates rectangular columnar (Col_r) mesophase over the temperature range 85–101 °C whereas a columnar hexagonal Col_h phase was observed in the temperature range 101–152 °C (Table 16). Good time-of-flight transients for both holes and electrons were demonstrated. A remarkably high values of hole mobilities of 0.20 $cm^2 \cdot V^{-1} \cdot s^{-1}$ and 0.10 $cm^2 \cdot V^{-1} \cdot s^{-1}$ were observed in the Col_r phase at 85 °C and in the Col_h phase at 100 °C, respectively. The values of electron mobility were equal to 0.30 $cm^2 \cdot V^{-1} \cdot s^{-1}$ in the Col_r phase at 85 °C and 0.20 $cm^2 \cdot V^{-1} \cdot s^{-1}$ in the Col_h phase at 100 °C [27, 91]. Since then, several α-alkylated phthalocyanines (**25-27**) (Table 15) have been synthesized and studied [92].

Table 15

Table 16

A summary of DSC data is presented in Table 16, while Fig. 14 shows typical optical polarizing micrographs. As shown in Fig. 14, compounds **25**, **26** and **27** display Col_h columnar mesophases. Compound **26** forms a crystalline phase of unexplained nature at temperatures between 112 and 124 °C which is lower than that for the Col_h phase. On comparing its optical texture (compare Fig. 14d with Fig. 14b and Fig. 14f) it was suggested that this compound is crystalline rather than LC. Furthermore, the film's texture shows clear difference from that of Col_r phase of compound **25** (see Fig. 14b). XRD data shows that compound **26** in its Col_h phase at 170-195 ^oC exhibits 110/200 diffraction peaks which correspond to a = 19.2 Å. A further broad band which corresponds to a d spacing of 3.5–5.0 Å was also observed. Cook and co-workers have studied compound **25** using XRD where they have observed a 110/200 peaks with a = 22.6 Å, a very weak 310 peak at ~13.0 Å, as well as a broad band which corresponds to a d spacing of 3.5-5.0 Å [90], however Bushby *et al* were unable to detect the weak 310 peak [92]. XRD measurements show that the compound **27** demonstrates crystalline phase at temperatures below 169 °C and is not columnar LC (Col_r) in nature [92].

Figure 14

Several examples of symmetrically tetra- and octa-substituted MPc mesogens have been described, where both alkyl and oligo(ethyleneoxy) side chains were used to induce MPc mesogenity. Geerts *et al* have synthesized liquid crystalline phthalocyanine bearing eight oligo(ethyleneoxy) substituents at peripheral positions (**28,** Table 4) to demonstrate an example

when the alignment of one and the same material can be switched by a simple change of a solid substrate from a hydrophilic to hydrophobic one [93, 94]. Typically, homeotropic alignment occurs during annealing at temperatures slightly below transition from the isotropic liquid to the LC mesophase, when the viscosity of the mesophase is the lowest. According to DSC and XRD data, **28** forms a rectangular columnar (Col_r) LC phase above 5 °C (enthalpy of crystalline/Col_r transition 16.1 kJ mol^{-1}) and shows hexagonal columnar phase (Col_h) upon heating transitions at 123 °C (1.2 kJ mol^{-1}) and then at 245 °C (3.7 kJ mol^{-1}) to the isotropic liquid.

Note that analogues of **28** bearing eight *n*-octyl or *n*-dodecyl ester groups do not show isotropic transition below decomposition temperature at 300 °C [93]. Hence, substitution of the alkyl chains by the $(CH_2CH_2O)_3Me$ groups is crucial to obtaining a material, which can be transformed into the isotropic liquid and, hence, is suitable for experimentation with homeotropic alignment. This effect is due to higher flexibility and, therefore, larger disorder of oligo(ethyleneoxy) chains compared to alkyl ones. When a film (5–20 μm in thickness) of phthalocyanine **28** was heated between two glass plates to 250 °C and then slowly cooled down, a homeotropic alignment of molecules was observed: in polarized optical microscopy (POM) experiments, the image appeared black between crossed polarizers (Fig. 15), whereas images taken between parallel polarizers have revealed digitated star-like structure, which is typical of Col_h phases [95-97].

Figure 15

3. Formation of Phthalocyanine films with planar alignment

3.1. Pseudoplanar M(II)Pc: Effect of substituents

The films of discotic liquid crystals are able to self-organize spontaneously and adopt a long-range oriented structure upon their heating to isotropic liquid, followed by slow cooling. Edge-on orientation of the disc-like molecules with the main columnar axis arranged parallel to the substrate surface is observed in thin films with planar (homogeneous) alignment. Analysis of the literature devoted to the alignment of the films of phthalocyanines M(II)Pc (M = 2H, Zn(II), Cu(II), Co(II), Ni(II) with long alkyl substituents shows that in most cases a planar alignment with the columnar directors randomly distributed in the plane parallel to the substrate surface is observed for films deposited on a substrate with the upper interface being air [98-100]. The film alignment is usually investigated by polarized optical microscopy. Fig. 16 shows a fan-like birefringent texture with extinction branches, which is indicative of edge-on orientation of MPc molecules. The bent columns of MPc molecules are centered on points indicated by the white crosses.

Figure 16

Similar POM textures were observed for annealed films of metal free and nickel phthalocyanines with oxygen-bridged laterally branched alkyl substituents (**1a, 1b, 10b, 10c)** spun on glass, ITO, PEDOT:PSS, Au as well as other substrates, with thicknesses ranging between 50-300 nm [98-100]. The planar columnar alignment was also studied in more details by the tapping-mode atomic force microscopy (TMAFM) of films spun onto a single glass substrate [98]. As-deposited films consisted of randomly distributed clusters or domains of columns with elongated shapes a few μm^2 in area. Such poorly ordered domains could be transformed into larger domains a few hundreds of μm^2 in area by heating the as-deposited films to the temperature of isotropic liquid followed by slow cooling. As a result much larger fan-like domains are formed with concentric stripes, along which the columns are aligned (see Fig. 17).

Figure 17

Thin films of compound **1b** 20 nm in thickness were produced by spin coating on the surface of doped silicon wafers [101]. Using a combination of X-ray absorption and photoelectron emission spectroscopies, the as-deposited films were shown to have areas with quite different degrees of macroscopic order. The order however appears to improve upon thermal annealing of these films. The orientation of spun films of **1b** (100 nm in thickness) was studied by TMAFM, employing ultra-fine tips with nanometer-thick whiskers [44]. The small-scale tapping mode amplitude image clearly shows the orientation of the columns with their axes lying parallel to the substrate surface, as shown in Fig. 18.

Figure 18

Fig. 18 was examined in details, specifically the orientation of columns near the domain boundaries. In some cases the columns are either laying parallel or making small angles with respect to the steps without causing any distorting the boundary structure (see arrows 1 and 2 in Fig. 18). In other instances the liquid crystalline domains were delimited by the step defects with different orientations of columns (see arrow 3 in Fig. 18). The columnar structure however remains undisturbed regularly by the domain boundaries; in other words, the columns assume continuity throughout the domains undisturbed by adopting a certain bend close to the boundary.

In organic thin film field effect transistors (OTFT), the formation of films of copper 1,4,8,11,15,18,22,25-octakis(hexyl)phthalocyanine aligned with the column axes parallel to the

substrate after annealing has resulted in improved device performance [102]. Similar to octasubstituted derivatives thin films of tetrasubstituted phthalocyanines M(II)Pc were characterized by planar alignment. For example, the molecule inclination angles of the phthalocyanine macrocycle relative to the substrate surface were determined from polarized Raman spectral measurements [99] to be 90^{o} for the compound **10c** (Table 1). Thin films of liquid crystalline peripherally-tetrasubstituted ZnPc derivative (**10b,** Table 1) were also prepared by spin coating and used as active layers in the fabrication of OTFTs. The latter exhibited significant increase in the field effect mobility as well as the on/off switching ratio in comparison with unheated films; this is mainly attributed to the planar alignment of molecules in their stacks within the annealed film which is more preferable for the transistor structures [103, 104].

DFT computations have been carried out by Wang and co-workers to study the effects of the length of alkyloxy substituents on the phthalocyanines self-assembling ability [105]. Stacking interactions of about 61.7 kcal/mol and 478.2 kcal/mol were computed for $CuPcOC_4$ and $CuPcOC_8$, respectively. Both stacking and in-plane interactions are comparatively strong in the case of $CuPcOC_8$ which supports the tendency of molecules of this compound to form self-assembled continuous films.

The introduction of sulfur-bridged alkyl (**11a**, **12a, 23)** [55, 67, 106, 107] and poly(oxyethylene) (**24**) [99] substituents into the phthalocyanine ring does not lead to the a significant change in the films alignment. Using polarized Raman spectroscopy, thin films of some octasubstituted phthalocyanines (e.g. **11a**, **12a** and **23** (Table 4)) with alkyl and alkoxy-substituents on the Pc ring were investigated [55, 67, 106, 107]. The films deposited on the surface of a single substrate (glass, Si, and ITO) with the upper air interface were characterised by a planar alignment with the columnar directors randomly distributed in the plane parallel to the substrate/air interface. Angle of molecule inclination changed from 75 to 90^{o} depending on the type of substituents while type of substituents show no effect on the orientation.

Preferential edge-on orientation of MPc macrocycles in films deposited on a single glass slide was also observed in films of M(II)Pc (M= Zn, Ni, Cu) (**3-5**) derivatives containing more complex substituents, namely monoazacrown ether moieties with long alkyloxyphenyl N-pivotal groups [53].

Following from the above results it can be concluded that planar alignment of Pc molecules can be realized by film deposition using the simple method of spin coating onto a single substrate followed by performing a regime of heat treatment. These results can be explained following work by Smela *et al* on calamitic liquid crystals, where the orientation of molecules on a single substrate was shown to be largely influenced by the surface tension forces at the LC-air interface [108]. These forces are significantly important in determining the

molecules orientation especially for films having thickness smaller than 30 μm. In this case the calamitic molecules are organized perpendicular to the substrate surface and their alkyl substituents point to the air. Following this argument interfacial forces occurring at the air-LC interface promote the planar molecular alignment since the surface tends to be composed only of alkyl substituents rather than aromatic cores. In the case of films deposited between two plates, the face-on anchoring of the disc-like molecules to the surface becomes predominant, and therefore homeotropic alignment is established.

Another important aspect which is worth mentioning is the influence of substrate surface on the alignment of M(II)Pc films. Substrates with different roughness and surface energy were characterised in terms of contact angles with water and hexadecane (Table 17).

Table 17

The measurements of contact angle with hexadecane was chosen because of hexadecane structural resemblance with the alkyl substituents in LC phthalocyanines. Films of MPc with alkoxy and alkyltio substituents display water contact angles in the range 65 to 90^o [109] typical of a hydrophobic surface. The increase of water contact angle of the initial disordered spun $CuPcR_8$ (**11b,** Table 4) film from 65 to 86.5^o after its thermal treatment [109] confirms the formation of films with planar alignment of columns in which the alkyl chains of substituents are directed outside. This value for water contact angle is identical to that of polyethylene [110] as was reported by Cupere and co-workers [98]. This indicates that the alkyl substituents control the interface properties of the substance. It is noteworthy mentioning here that the values of the substrates contact angles with hexadecane fall in a very narrow interval (from 5° for PCBM to 12° for PEDOT:PSS). This indicates to insensitivity of alkyl chains to the substrate material and explains similar orientation of phthalocyanine films on different substrates. A different behavior is observed for FKM substrate having fluorinated moieties. However for deposition of ultrathin films or at the interface between the substrate and the bulk phase the role of substrate can be important. A substrate-induced phase was found at the interface between the bulk phase of 2(3),9(10),16(17),23(24)-tetra(2-decyltetradecyloxy)-phthalocyanine films and the Si/SiO*x* substrate [111]. On the basis of XRD, Grazing Incidence X-ray Diffraction (GIXD) and AFM a model structure of the substrate-induced phase (~30 nm in thickness) was proposed. That phase named *columnar tetragonal crystal plastic phase* consisted of a centered tetragonal lattice with macrocycles of adjacent phthalocyanine molecules rotating by 45° along the columnar axis. Note that the tetragonal lattice of the substrate-induced phase is incommensurate with the rectangular lattice of the contact bulk phase [112].

Most discotic M(II)Pc (M = 2H, Cu, Co, Ni, Zn) give films with a random planar alignment of columns in which the directors are arranged parallel to the surface but azimuthally disordered, on the surface of one substrate independently on the phthalocyanine molecular structure and substrate material. For practical applications (e.g. in OFET) it is important to obtain films with uniaxial planar alignment in order to create the preferred conduction channel between electrodes. The special approaches for the formation of phthalocyanine films with uniaxial planar alignment are discussed below.

3.2. Shuttle-cock shaped and double-decker phthalocyanines

Most M(II)Pc described in the pevious section have a pseudoplanar geometry while Pb(II) phthalocyanines have a unique shuttle-cock shaped structure, where the position of Pb atom deviates by 0.37–0.40 Å from the phthalocyanine macrocycle plane [113]. Similar to substituted phthalocyanines with planar geometry, octakis and tetrakis (alkylthio)-substituted Pb(II) phthalocyanines also form columnar mesophases over a wide temperature range [36, 69, 72, 114]. The alignment of liquid crystalline films of lead phthalocyanines (**13a, b** (Table 4), **14**, **15** (Table 1)) were studied in the literature [72, 74]. IR spectra of thin films of compounds **13a,b**, **14**, and **15** have revealed an increase in the intensity of the out-of-plane vibrations in comparison with in-plane ones. This increase was associated with an edge-on preferential orientation of PbPc macrocycles on the surface [72].

Another interesting example of the phthalocyanine with shuttle-cock shaped structure is LC tetraoctylsubstituted vanadyl phthalocyanine derivative. Spin coating of its solution results in the formation of aligned films with edge-on orientation of MPc molecules after heating at 120 ^{o}C with a field effect mobility of 0.017 cm^2V^{-1} s^{-1}[115].

The films of bis[octakis(hexylthio)phthalocyaninato] rare-earth metal(III) complexes $[(C_6S)_8Pc]_2M$ (M=Gd(III), Dy(III), and Sm(III)) (Compounds **19-22** (Fig. 10)) deposited onto the surface of a single glass or silicon substrate also exhibit planar alignment after slow cooling of their isotropic melts [77].

The orientation of films deposited on a surface when the second interface is air is independent of the molecular structure of phthalocyanine and type of substituents in the MPc ring. However the type of substituents in $PbPcR_8$ macrocycle can influence on the size of the oriented domains. Comparison of phthalocyanines bearing substituent of different length allows us to conclude that more continuous films with larger domains form in the case of phthalocyanines with longer alkyl substituents. Therefore, thin films of $PbPcR_8$ with R=-$S(CH_2)_{15}CH_3$ (**13b,** Table 4) exhibit larger domains than in the case of $PbPcR_8$ with R=-

$S(CH_2)_7CH_3$ (**13a**) deposited onto similar glass substrates after slow cooling from isotropic melt (Fig. 19).

Figure 19

3.3. Special approaches for deposition of phthalocyanine films with uniaxial planar alignment

3.3.1. Modification of substrate surface

Creation of special patterns on the substrate surface is one of several approaches for the deposition of oriented films of LC materials. Patterns of different sizes can be created by traditional rubbing as well as using more sophisticated techniques for micrometer-scale patterning. The rubbing of polymers is very simple technique and it is widely used even for production of substrates for liquid crystalline displays.

Cattle *et al* used an epoxy side-chain substituted poly(methylenephenylene) (SU8) cross-linked under UV irradiation for creation of microchannels with widths from 2 to 25 μm (Fig. 20) [116]. Using capillary forces, the channels were filled with melted discotic phthalocyanines (Compounds **25-27,** Table 15) with the subsequent slow cooling down to the Col_h phase.

Figure 20

POM measurements for the three LC phthalocyanines **25–27** shows that the films exhibited planar alignment with the column directors lying across the channels (Fig. 21). The alignment across the channels was induced by homeotropic anchoring at the SU8 polymer interface. The film alignment depends on the channel width; the narrower channels the easier the LC alignment, however this alignment is also dependent on the phthalocyanine molecular structure (Table 18).

Figure 21

Table 18

The other method for creation of a bidimensional network of well ordered LC phthalocyanine films (Compound **1b,** Table 1) was demonstrated for compound **1b** as an example by Mouthuy and co-workers [117, 118]. Using e-beam lithography and utilizing poly(methylmethacrylate) mask a set of parallel groove 200 nm wide were fabricated followed by etching the underlying oxidized silicon wafer to a depth of 30 nm. The wafer was then spin-casted with a solution of compound **1b** in hexadecane to fill-in the grooves. With a proper design of the template geometry this technique is based on controlling the anisotropic interfacial tension between the

discotic columns and the nanogrooves walls forcing the columns to align in specific directions. Mouthuy *et al* have been successful in obtaining a uniaxial alignment of the columns via confining the discotic phthalocyanine molecules in a network of intersected nanogrooves [117, 118].

3.3.2. Chemically Patterned Surfaces

Chemically patterned surfaces are also used to deposit films of discotic LCs with uniaxial planar alignment. The method of microcontact printing of organothiol monolayers was used in the work of Bramble *et al* [119] for chemical patterning of gold surface. The other approach was based on deep UV patterning of organosilane self assembled monolayers on silicon (Fig. 22). Compound **25** (Table 15) has two discotic LC phases, Col_h phase formed above 101 ^oC and Col_r formed above 85 ^oC. Compound **25** in Col_h phase formed the films with planar alignment with the directors lying parallel to the stripe direction.

Figure 22

Two distinct planar orientations were observed upon cooling the film of **25** to the Col_r mesophase [119]. These two orientations were formed because the discotic molecules are tilted relative to the director.

3.3.3. Alignment by zone casting and mechanical shearing

The LC phthalocyanine films with uniaxial orientation of columns can be deposited by mechanical shearing [120, 121]. A zone casting technique also gives highly oriented phthalocyanine films in which the columnar axes lie perpendicular to the film growth direction [122]. In this method, a solution of the discotic phthalocyanine was dispensed in a continuous manner via a flat nozzle onto a slowly moving substrate. A meniscus is formed between the moving substrate and this nozzle and as a result of concentration gradient within the meniscus the solute solidifies within a narrow zone along the edges of the meniscus (Fig. 23). Anokhin *et al* [123] were studied the structural differences of the 2(3),9(10),16(17),23(24)-tetra(2-decyltetradecyloxy)-phthalocyanine (**1b**) films deposited by zone-casting and mechanical shearing.

Figure 23

The columnar axes of the **1b** films deposited by the mechanical shearing method were mainly oriented along the shearing direction, but their planar orientation was not perfect. On the other

hand the columnar axes in the films obtained by zone casting were oriented perpendicular to the casting direction and the produced films were smooth and more regular containing large co-facial aggregates of **1b** molecules. In this method the density of the oriented domains is largely determined by process parameters including solution concentration, type of solvent, distance between the substrate and the nozzle, the substrate withdrawal rate [122]. Doctor blade casting at room and elevated temperatures was also demonstrated for the preparation of films of the phthalocyanine **7b** (Table 4) with azimuthal anisotropy [124].

3.3.4. Magnetic and electric field effects

The first work on magnetic and electric field effects on the alignment of discotic Pc LCs was reported by Z. Belarbi in 1990 [125]. The alignment of discotic molecules can be controlled by application of external electric [126] or magnetic field [127]. Using 4 wt.% cobalt porphyrazine derivative in hexane solution, alignment of this LC material on a substrate upon gradual solvent evaporation under applied constant magnetic field (H=0.7 T) was examined by small angle neutron scattering (SANS) [128]. SANS pattern of the drop casted porphyrazine film revealed strong anisotropy, demonstrating a clear indication of columnar axes alignment perpendicular to the magnetic field vector. Fig. 24 shows an illustration of the columnar alignment relative to the magnetic field direction. A similar procedure was used by Kim *et al* to produce uniaxially oriented films of columnar cobalt 2,3,7,8,12,13,17,18-octa(n-dodecylthio)porphyrazine over large scale (centimeter scale) area without relying on substrate effects [128].

Figure 24

SANS as well as cryo-TEM data show that this approach employs the diamagnetic interaction between the aromatic macrocycles of discotic LCs and under applied magnetic field in the range 0.4-1.1 T. The sample was continuously spun in the presence of the magnetic field whilst the film was cooled from isotropic melt to LC phase. With the rotation speed more suitable for the alignment as low as 5–10 rpm, porphyrazine derivative formed aggregates with uniaxial columnar alignment, in which the columnar directors were parallel to the rotation axis which in its turn was perpendicular to the magnetic field vector [129].

Direct current (dc) electric field alignment of self-assembled nanofibers of the compound **7e** (Table 4) in dodecane solution was investigated using experimental cells of indium-tin oxide coated glass slides separated by an insulating cover glass of 150 μm in thickness assembled with epoxy. As soon as the floating nanofibers come to contact with the ITO substrate, they adhere to it in a planar way when the electric field is absent. However when the electric field is turned on,

the nanofibers are oriented perpendicular to the ITO surface with their long axis lying parallel to the electric field [130].

4. Formation of Phthalocyanine films with homeotropic alignment

4.1. Films confined between two substrates and electrodes

4.1.1. Influence of phthalocyanine molecular structure and the substituents type on films alignment

Geerts *et al* [98] have examined the influence of confinement between two substrates in the formation of homeotropically aligned thick and thin films of **1b** derivative (Table 1) with oxygen-bridged laterally branched alkyl substituents. Thin (a few tens of nanometers) films were deposited by spin-coating of the appropriate solutions. Thick films (a few micrometers) were obtained by melting **1b** between two different or identical substrates. For this purpose a small amount of MPc on a bottom substrate was heated at a temperature about 20 °C above the clearing point, followed by placing a top substrate on the molten LC. Then a slight pressure was applied in order to spread the film on the largest possible area and the confined film was slowly cooled down. The same techniques was followed for the deposition of thin films between quartz and KBr slides [99]. The films (0.3-3 μm) of tetrasubstituted phthalocyanines M(II)Pc$(OR)_4$ (e.g. compound **10c** (Table 1)) confined between two identical plates (KBr or quartz) were studied by polarized optical microscopy and polarized Raman spectroscopy. In contrast to planar alignment exhibiting a highly birefringent texture, homeotropically aligned films of phthalocyanines in Col_h phase demonstrate the absence of texture [98, 99]. The appearance of the dark image (Fig. 25) in the case of homeotropic alignment is because the optical axis is parallel to the columnar axis [131].

Figure 25

Similar optical observations of the films of **1b** have been made between ITO, Au substrates and slides covered with PEDOT: PSS, PCBM, and poly(isobutylene) polymers [98] as well as between two glass slides [132]. The films of **1b** in the Col_r phase at 40 ^oC became dark blue with bright straight lines when observed with POM because of some slight defects which can be caused by the biaxiality of the Col_r phase.

Deibel and co-workers have demonstrated an example of real electronic device application of **1b** films with homeotropic alignment [133]. In this example they have confined compound **1b** between two parallel ITO electrodes separated by SiO_2 beads (3-5 μm in

diameter). Such molecular alignment is useful for the formation of active layers of organic solar cells and light-emitting diodes.

As in the case of films deposited on the surface of one substrate the introduction of sulfur-bridged alkyl (**11b, 13a,b)** [68, 73] and poly(oxyethylene) (**24**) [134] substituents into the phthalocyanine ring did not lead to a significant change in the films alignment in comparison with phthalocyanines having –OR substituents. Using Raman spectroscopy as well as polarized optical microscopy, the orientation of tetra-substituted nickel phthalocyanine (Compound **24**) films deposited between two substrates [99] or between two electrodes for electronic device applications [134] was extensively investigated. Thin films of compound **24** were deposited on ITO-coated glass slides, which were used as bottom electrodes followed by the deposition of gold or aluminum films using physical vapor deposition (PVD) as top electrode employing a purpose-constructed mask (see Fig. 26). Tetra-substituted nickel phthalocyanine films confined between two glass substrates as well as between bottom and top electrodes exhibit homeotropic alignment; this type of alignment however was not observed when the films were deposited on ITO-coated slide with air representing the upper interface. The annealing of the films confined between two electrodes leads to homeotropic alignment which improves charge transport along the main axis in the columns oriented perpendicular to the electrodes [134].

Figure 26

Thermally induced orientation in copper octakisalkylthiophthalocyanine (Compound **11b**) films confined between ITO and Al electrodes was studied by Basova *et al* [68] by the methods of spectral ellipsometry, UV-visible and polarized Raman spectroscopies. Annealing produces alignment of the films which were disordered before heating. After heat treatment the films exhibited homeotropic alignment with phthalocyanine molecules oriented practically parallel to the electrode surface as confirmed by the estimation of the inclination angles of molecules using polarized Raman spectroscopy. The films' conductivity increases by one order of magnitude as a consequence of such structural changes.

Depending on the length of alkyl substituents ($–SC_8H_{17}$ and $–SC_{16}H_{33}$), thin films of nonplanar lead phthalocyanine derivatives (Compounds **13a,b**) [73] confined between ITO and indium electrodes demonstrate different alignments. In accordance with the data of polarized Raman spectroscopy and polarized optical microscopy (POM) thin films of compounds **13a** and **13b** with alkylthio substituents confined between two electrodes exhibited homeotropic alignment at room temperature while their analogues with alkoxysubstituents [73] did not show homeotropic alignment. Different behavior of the alkoxy substituted analogues appeared to be associated with their higher melting points and higher viscosity at room temperature. Note that

the alignment of molecules of shuttle-cock shaped phthalocyanines and bisphthalocyanines in thin films confined between two substrates or electrodes is similar to that observed for thin films of phthalocyanines having pseudoplanar structure. As an example, the conductivity of dysprosium bisphthalocyanine (**21**) film deposited between ITO and Al electrodes in LC state measured at 350 K was 2 orders of magnitude higher in comparison with the same film in crystalline state which clearly suggests the homeotropic alignment of the film in LC state [135].

The example of the formation of homeotropically aligned film of non-peripherally octasubstituted H_2Pc (**25**) is worth highlighting [91]. An experimental cell composed of two ITO-coated slides separated by ~25 μm PET spacers was filled with the LC phthalocyanine **25** by capillary action at about 170 °C. The mobility of the formed homeotropically aligned films with the columns oriented perpendicular to the electrode was studied using space-charge limited current and time-of-flight photoconductivity measurements. The mobility along the columnar axis of **25** has attained values up to $2.8x10^{-3}$ cm^2/Vs, while it was about 2 orders of magnitude lower in the case of transport perpendicular to the columnar axis [91].

The introduction of bulky aromatic substituents into the macrocycle lends peculiar properties to the phthalocyanine molecule and has an impact on the behavior of phthalocyanines on the substrate surface. Generally, LC phthalocyanines have high viscosity and give multidomain films with disclinations and many boundaries between these domains. Hatsusaka *et al* demonstrated the first example of phthalocyanine derivatives of the octakis(dialkoxyphenoxy)-phthalocyaninatocopper(II) complexes (Compounds **6a-f** (Table 4)) exhibiting Col_{tet} mesophase and spontaneously forming films with uniform homeotropic alignment between quartz or soda-lime glass plates [56]. Formation of the homeotropically aligned films without defects and domain boundaries was explained by low viscosity of isotropic melts of **6a-f** which was associated with the introduction of oxygen atoms into the substituents [136].

Although MPc derivatives A (Fig. 27) strongly resemble the MPc derivatives B used by Hatsusaka *et al* [56], they do not show homeotropic alignment. The main difference between A and B structure is oxygen bridge atoms between the phthalocyanine macrocycle and phenyl groups. Therefore, the presence of oxygen atoms explains the homeotropic alignment in the case of derivative B. The parallel orientation of MPc macrocycles is induced by the stronger interaction between lone pairs of oxygen atoms of the phenoxy group and dangling bonds of Si atoms on the quartz or glass surfaces (Fig. 27). The MPc molecules of the first layer, attached to the surface, triggered the stacking of MPc molecules of the next layers [56, 137].

Figure 27

This hypothesis was also supported by another example described in the literature [138] for thin films of tetrakis(2,3,6,7-tetraalkoxy)-triphenylenocyaninato copper(II) (Fig. 28a) and tetrakis(2,3,6,7-tetraalkoxy)-1,4-diazatriphenylenocyaninato copper(II) (Fig. 28b). Compound **29** does not form homeotropically aligned films, whereas compound **30** in the Col_{tet} mesophase demonstrates spontaneous homeotropic alignment. The only difference between these two compounds is eight nitrogen heteroatoms in the compound **30**. Hence, the introduction of heteroatoms like nitrogen may also facilitate the formation of MPc films with perfect homeotropic alignment.

Figure 28

MPc-C60 dyads with M = Cu, Co and Ni (Fig. 29) are also able to form the homeotropically aligned films for the highest temperature Col_{tet} mesophase [139, 140].

Figure 29

4.1.2. Influence of the mesophase type on the films alignment

An interconnection between the alignment behavior and mesophase type has been demonstrated by Schweicher and co-workers [141]. They studied the films of two miscible phthalocyanines possessing different thermotropic behavior and their blend, deposited on the surface on one substrate and confined between two substrates; compound **31** (Table 4) showed Col_r-isotropization at 151.6 ^oC (8.18 kJ mol^{-1}), while compound **32** (Table 1) demonstrated a Col_r-Col_h transition at 58.3 ^oC (0.07 kJ mol^{-1}) as well as Col_h-I transition at 181.6 ^oC (4.8 kJ mol^{-1}) [43, 93, 142]. Col_h and/or Col_{tet} mesophases favor homeotropic alignment while Col_r mesophase induces planar alignment. In fact, the arrangement of phthalocyanine macrocycles within the column is dissimilar in Col_h and in Col_r mesophases, *viz* a face-to-face arrangement with no tilt relative to the columnar axis is presented in Col_h mesophase, while a slight tilt is observed in Col_r mesophase. It is therefore clear that only Col_h mesophase is able to form columns strictly perpendicular to the substrate surface whereas only pseudohomeotropic alignment can be observed in the case of Col_r phase if specific interactions between substrate and LC phthalocyanine molecules is absent.

4.1.3. Influence of the substrate material

Influence of the substrate materials on the formation of the films is described by Cupere *et al* [98]. The authors have shown that the substrate material had negligible effect on the film

alignment, however in some cases substrate influence was observed. For instance, some substrates such as FKM (see Table 17) did not induce a specific molecular alignment [98].

Liquid crystalline phthalocyanine (Compound **28**) bearing eight oligo(ethyleneoxy) peripheral substituents gives homeotropically aligned films (5–20 μm thickness) between two glass substrate with hydrophilic surfaces, whereas random planar alignment forms between two hydrophobic plates coated by benzocyclobutene-based crosslinked polymer (obtained by the thermal annealing of divinylsiloxane-bis-benzocyclobutene [97]. This difference in alignment behavior apparently originates from different interactions between the substrate and the peripheral chains of MPc molecules. H-bonding between oligo(ethyleneoxy) substituent chains and residual hydroxy groups on a hydrophobic substrate induces the *face-on* orientation of molecules of the first layer. *Edge-on* orientation of the MPc macrocycles with the substrate however takes place if such interactions do not occur on the cross-linked polymer surface.

4.1.4. Influence of film thickness

When films are confined between two substrates the film thickness (a few nanometer compared to a few micrometer thick films) plays a major role in the process of discotic molecules reorganization upon heating. For thick films to exhibit homeotropic alignment they need to be heated to the temperature of the isotropic phase and then slowly cooled down. In this case the substrate is providing sufficient anchoring force for the discotic molecules to align over small distances, however, an additional major decrease in the viscosity of the phthalocyanine is required in the case of thick films (micrometers in thickness) to assist the generation of the surface-induced ordering throughout the entire film thickness. Similar to LC benzoperylene derivatives [143, 144] phthalocyanine films with a very small thickness align more easily when sandwiched between two solid substrates. In some cases thin films have to be annealed just below the clearing point. With film thickness increasing the films have to be cooled down from isotropic melt much more slowly. However full alignment of molecules in the film is often extremely difficult to achieve if the film thickness is larger than a few tens of micrometers.

4.2. Special approaches for deposition of homeotropically aligned phthalocyanine films on the surface of a single substrate

As described in Section 4.1, the confinement of LC phthalocyanines between two substrates leads to the formation of films with homeotropic columnar arrangement. It is very important to develop methods which allow the deposition of films with homeotropic alignment not only between two solid surfaces but also on a single substrate. The films usually keep homeotropic alignment even after the separation of the two plates, however this alignment can be kept only

until annealing is applied to MPc films after separation [98]. This method of separation of the two plates cannot be used for preparation of smooth and uniform films. However the use of an upper substrate as a confinement layer is not applicable for deposition of thin MPc films spun on one glass plate because of the lack of contact between the upper substrate and thin phthalocyanine film. In this case a sacrificial layer spun on top of the LC layer can be used as the second confinement layer. To avoid the washing-off the MPc layer, appropriate solvents must be used for deposition of the sacrificial layer. After annealing the sacrificial layer can be gently removed by a simple washing. The use of a polymer (e.g. poly(vinylphenol)) as a sacrificial layer induces homeotropic alignment of **1b** [145] (Fig. 30).

Figure 30

Similarly to the films confined between two plates, the films confined by a sacrificial layer was shown by the methods of optical microscopy, UV-vis spectroscopy, AFM, and grazing incidence wide angle X-ray scattering to be aligned with face-on orientation of macrocycles on the substrate surface. This occurred well below the isotropization temperature for the 50-300 nm thick films of **1b**. Homeotropic alignment was maintained after washing of the sacrificial layer with methanol, however subsequent re-annealing of the film led to the formation of the films with edge-on orientation of MPc molecules [145].

The other important approach for the deposition of homeotropically aligned MPc films on the surface of a single substrate is basen on the strong specific interaction between MPc molecules and the surface [146-148]. Such a specific interaction can be achieved both through the central metal and through the substituents in the phthalocyanine ring. The chemisorption method was used to prepare self assembled monolayers (SAMs) of manganese(III) phthalocyanine complexes ($MnClPc(SR)_8$ (R = n-C_8H_{17} and n-$C_{12}H_{25}$)) onto gold-coated substrates. Although the liquid crystalline transitions of these compounds were not studied, the authors however have discussed their mesogenic nature. Using XPS, NEXAFS and ToF-SIMS these SAMs were characterized showing the formation of well-defined homogeneous monolayers [146]. The constituents of these SAMs were bonded to the substrate surface via thioether coordination chemistry. Phthalocyanine aromatic cores show quite good orientational order whereas the long chains are mostly disordered. Data analysis of Near Edge X-Ray Absorption Fine Structure (NEXAFS) spectroscopy measurements shows good consistency with discotic molecules orientation mainly parallel to the substrate surface.

The other very useful approach to obtain homeotropic aligned films onto single substrate is the anchoring of the molecules using special tunable command layers. Hoogboom and co-authors [147, 148] have reported on a modification of ITO substrate by using pyridine-

functionalized siloxane as a command layer (Fig. 31). This results in the formation of a homeotropically aligned layer due to the binding of zinc phthalocyanine **7d** (Table 4) through the coordination of nitrogen atoms of the pyridine groups to the zinc centers. A surface-templated epitaxial growth of perpendicular colums of **7d** molecules was initiated by this coordination.

Figure 31

Under similar conditions, the metal-free phthalocyanine analogue did not attach to the pyridine-containing command layer and was easily come off completely using chloroform. This experiment confirms the assumption that coordinative binding between ZnPc molecules and the functional groups of the command layer was required. The size of the aligned ZnPc aggregates formed during this surface-templated growth was controlled by varying the immersion time.

The films of azacrown substituted phthalocyanines **2** and **3-5** (Fig. 3) with homeotropic alignment of molecular columns were obtained on NaCl substrate surface [47, 53]. In that case the specific interaction was due to the ability of monoazacrown ether groups to coordinate sodium ions of NaCl substrate. The other crown ether-substituted phthalocyanine gave the homeotropic alignment on the basal plane of graphite substrate [149].

5. Summary

An overview of films' growth of mesogenic MPcs offering systematic analysis of the influence of different factors on the structural organization of liquid crystalline phthalocyanine films, including regimes of heating, substrate materials, type of interfaces and phthalocyanines molecular structure was provided in this review. The literature analysis allows to determine some regularities of the formation of ordered phthalocyanine films.

Spontaneous alignment of liquid crystalline phthalocyanines strongly depends on the air-liquid crystal interface. Mesogenic phthalocyanines form homeotropically aligned films when sandwiched between two substrates, while they gives planar alignment on the surface of a single substrate. The surface tension of low rough solid substrates has negligible effect on the film alignment.

Analysis of the structure of the films of metal phthalocyanines with various substituents (R = $-SC_nH_{2n+1}$, $-OC_nH_{2n+1}$, $-OCH_2CH(C_{12}H_{25})-(C_{10}H_{21})$, $-S(CH_2O)_nCH_3$, $-OPh(C_nO)_2$ etc.) deposited on a single substrate allows us to conclude that the type of substituents play no role in influencing molecular alignment if specific interactions between substrate and LC phthalocyanine molecules is absent. The introduction of sulfur atoms as bridge atoms between phthalocyanine macrocycle and alkyl chain or introduction of additional ether oxygens to the

alkyl chains resulting in an increase of the transition temperature to isotropic liquid due to stronger intermolecular between substituents of the adjacent molecules does not result in a change in the alignment of the films deposited on a single substrate. The type of substituents however can influence the size of the oriented domains. Comparison of phthalocyanines bearing substituent of different lengths allows us to conclude that more continuous films with larger domains are formed in the case of phthalocyanines with longer alkyl substituents. The alignment of molecules of shuttle-cock shaped phthalocyanines and bisphthalocyanines in thin films is similar to that observed for thin films of phthalocyanines having pseudoplanar structure.

Most discotic phthalocyanines give films with a random planar alignment of columns in which the directors are oriented parallel to the surface but azimuthally disordered independently on the phthalocyanine molecular structure and substrate material. Special approaches for the formation of phthalocyanine films with uniaxial planar alignment are required; these for instance are achieved via films' deposition onto patterned surfaces, alignment by mechanical shearing and zone casting, and so on.

The confinement of LC phthalocyanines between two plates leads to the formation of the films with a homeotropic columnar arrangement. For many LC phthalocyanines, the molecular structure proves much more significant in determining the homeotropic alignment obtained. One of the manners to induce the homeotropic alignment between two substrates is to modify the substituents in phthalocyanine ring, e.g. by introducing more ether oxygens that promote face-on anchoring of MPc molecules on high-energy surfaces. The films with the homeotropic alignment on the surface of a single substrate can also be achieved using a polymer sacrificial layer which can be removed after the film annealing or special tunable command layer which provide strong specific interaction between its functional groups and the phthalocyanine molecules.

Acknowledgements

Analysis of the literature on investigation of the influence of different factors in the structural organization of liquid crystalline phthalocyanine films as well as on achievements in the development of the methods for the formation of liquid crystalline phthalocyanine films with controllable alignment and ordering was carried out under the financial support of the Russian Scientific Foundation (project N 15-13-10014). The Scientific and Technological Research Council of Turkey (TUBITAK) and the Gebze Technical University are gratefully acknowledged for their support of the research of liquid crystalline properties of phthalocyanines.

References

1. B. Simic-Glavaski, in C.C. Leznoff, A.B.P. Lever (Eds.), Phthalocyanines. Properties and Applications. Vol. 3, VCH (LSK), Cambridge, 1993, pp. 119-166.

2. G. de la Torre, M. Nicolau, T. Torres, in: H.S. Nalwa (Ed.), Supramolecular Photosensitive and Electroactive Materials, Academic Press, 2001.

3. J. Barbera, in: J.L. Serrano (Ed.), Metallomesogens. Synthesis, Properties and Applications, VCH, Weinheim, 1996.

4. J. Simon, P. Bassoul, in C.C. Leznoff, A.B.P. Lever (Eds.), Phthalocyanines. Properties and Applications, Vol. 2, VCH (LSK), Cambridge, 1993, pp. 223-299.

5. M. Hanack, D. Dini, in: K.M. Kadish, K.M. Smith, R. Guilard (Eds.), The Porphyrin Handbook. V. 18, San Diego, CA: Academic Press, 2000, pp. 251-280.

6. M.J. Cook, I. Chambrier, in K.M. Kadish, K.M. Smith, R. Guilard (Eds.), The Porphyrin Handbook , V. 17, San Diego, CA: Academic Press, 2000, pp.37-128.

7. A.M. van de Craats, N. Stutzmann, O. Bunk, M.M. Nielsen, M. Watson, K. Müllen, H.D. Chanzy, H. Sirringhaus, R. Friend, Adv. Mater. 15 (2003) 495-499.

8. P. Peumans, A. Yakimov, S.R. Forrest, J. Appl. Phys. 93 (2003) 3693-3723.

9. L. Schmidt-Mende, A. Fechtenkötter, K. Müllen, E. Moons, R.H. Friend, J.D. MacKenzie, Science 293 (2001) 1119-1122.

10. S. Wang, Y.Q. Liu, X.B. Huang, S.L. Xu, J.R. Gong, X.H. Chen, L. Yi, Y. Xu, G. Yu, L.J. Wan, C.L. Bai, D.B. Zhu, Appl. Phys. A: Mater. Sci. Process. 78 (2004) 553-556.

11. A.J. Ikushima, T. Kanno, S. Yoshida, A. Maeda, Thin Solid Films 273 (1996) 35-38.

12. C. Chu, V. Shrotriya, G. Li, Y. Yang, Appl. Phys. Lett. 88 (2006) 153504.

13. I. Seguy, P. Destruel, H. Bock, Synth. Met. 15 (2000) 111-112.

14. L. Valli, Adv. Col. Interface Sci. 116 (2005) 13-44.

15. M.L. Rodriguez-Mendez, J. Souto, R. de Saja, J. Martinez, J. A. de Saja, Sens. Actuat. B 58 (1999) 544-551.

16. S. Mohnani, D. Bonifazi, Coord. Chem. Rev. 254 (2010) 2342-2362.

17. H. Peisert, I. Biswas, M. Knupfer, T. Chassé, Phys. Status Solidi B 246 (2009) 1529-1545.

18. M.J. Cook, Pure Appl. Chem. 71 (1999) 2145-2151.

19. S. Palacin, Adv.Colloid Interface Sci. 87 (2000) 165-181.

20. C. Piechocki, J. Simon, A. Skoulios, D. Guillon, P. Weber, J. Am. Chem. Soc. 104 (1982) 5245-5247.

21. S. Sergeyev, W. Pisula, Y.H. Geerts, Chem. Soc. Rev. 36 (2007) 1902-1929.

22. R.J. Bushby, K. Kawata, Liq. Cryst 38 (2011) 1415-1426.

23. R. Cristiano, H. Gallardo, A.J. Bortoluzzi, I.H. Bechtold, C.E.M. Campos, R.L. Longo, Chem. Commun. 2008, 5134-5136.
24. J.M. Warman, M.P.de Haas, G. Dicker, F.C. Grozema, J. Piris, M.G. Debije, Chem. Mater. 16 (2004) 4600-4609.
25. Z. An, J. Yu, S.C. Jones, S. Barlow, S. Yoo, B. Domercq, P. Prins, L.D.A. Siebbeles, B. Kippelen, S.R. Marder, Adv. Mater. 17 (2005) 2580-2583.
26. B.A. Jones, M.J. Ahrens, M.-H. Yoon, A. Facchetti, T.J. Marks, M.R. Wasielewski, Angew. Chem. Int. Ed. 43 (2004) 6363-6366.
27. H. Iino, Y. Takayashiki, J.-I. Hanna, R.J. Bushby, Jpn. J. Appl. Phys. 44 (2005) L1310-L1312.
28. W. Pisula, A. Menon, M. Stepputat, I. Lieberwirth, U. Kolb, A. Tracz, H. Sirringhaus, T. Pakula, K. Mullen, Adv. Mater. 17 (2005) 684-689.
29. C.D. Simpson, J. Wu, M.D. Watson, K. Mullen, J. Mater. Chem. 14 (2004) 494-504.
30. G. Lussem, J.H. Wendorff, Polym. Adv. Technol. 9 (1998) 443-460.
31. E.-K. Fleischmann, R. Zentel, Angew. Chem. Int. Ed. 52 (2013) 8810-8827.
32. S. Kumar, Chem. Soc. Rev. 35 (2006) 83-109.
33. M. Victoria Martínez-Díaz, G. Bottari, J. Porphyrins Phthalocyanines 13 (2009) 471-480.
34. K. Ohta, H.-D. Nguyen-Tran, L. Tauchi, Y. Kanai, T. Megumi, Y. Takagi, in: K.M Kadish, K.M. Smith, R. Guilard (Eds.), Handbook of Porphyrin Science, V. 12, World Scientific, 2011, pp.1-120.
35. M.K. Engel, P. Bassoul, L. Bosio, H. Lehmann, M. Hanack, J. Simon, Liq. Cryst. 15 (1993) 709-722.
36. M. Hanack, A. Beck, H. Lehmann, Synthesis 8 (1987) 703-705.
37. I. Cho, Y. Lim, Mol. Cryst. Liq. Cryst. 154 (1988) 9-26.
38. J.F. van der Pol, E. Neeleman, J.W. Zwikker, R.J.M. Nolte, W. Drenth, J. Aerts, R. Visser, S.J. Picken, Liq. Cryst. 6 (1989) 577-592.
39. W.T. Ford, L. Sumner, W. Zhu, Y.H. Chang, P.-J. Um, K.H. Choi, P.A. Heiney, N.C. Maliszewskyj, New J. Chem. 18 (1994) 495-505.
40. N.B. McKeown, Phthalocyanine Materials: Synthesis, Structure and Function, University Press, Cambridge, UK, 1998, pp. 60-80.
41. C. Rager, G. Schmid, M. Hanack, Chem. Eur. J. 5 (1999) 280-288.
42. B. Görlach, M. Dachtler, T. Glaser, K. Albert, M. Hanack, Chem. Eur. J. 7 (2001) 2459-2465.

43. J. Tant, Y. H. Geerts, M. Lehmann, V. De Cupere, G. Zucchi, B. W. Laursen, T. Bjørnholm, V. Lemaur, V. Marcq, A. Burquel, E. Hennebicq, F. Gardebien, P. Viville, D. Beljonne, R. Lazzaroni, J. Cornil, J. Phys. Chem. B 109 (2005) 20315-20323.
44. R.I. Gearba, A.I. Bondar, Goderis, B.; Bras, W.; Ivanov, D. A. Chem. Mater. 17 (2005) 2825-2832.
45. J. Barbera, O.A. Rakitin, M. Blanca Ros, T. Torroba, Angew.Chem. Int. Ed. 37 (1998) 296-299.
46. M. Suarez, J.-M. Lehn, S.C. Zimmerman, A. Skoulios, B. Heinrich, J. Am. Chem. Soc. 120 (1998) 9526-9532.
47. T.V. Basova, I.V. Jushina, A.G. Gürek, D. Atilla, V. Ahsen Dyes Pigments, 80 (2009) 67-72.
48. C. Sirlin, L. Bosio, J. Simon, V.Ahsen, E.Yılmazer, Ö.Bekâroğlu, Chem. Phys. Lett. 139 (1987) 362-365.
49. V. Ahsen, A.G. Gürek, E. Musluoğlu, A. Gül, Ö. Bekaroğlu, Chem. Ber. 122 (1989) 1073-1074.
50. M. Kandaz, Ö. Bekaroğlu, J Porphyrins Phthalocyanines 3 (1999) 339-345.
51. B. Cabezon, E. Quesada, S. Esperanza, T. Torres, Eur. J. Org. Chem. 15 (2000) 2767-2775.
52. D. Atilla, V. Ahsen, J. Porphyrins Phthalocyanines 6 (2002) 593-596.
53. T.V. Basova, F. Latteyer, D. Atilla, A.G. Gürek, A.K. Hassan, V. Ahsen, H. Peisert, T. Chassè, Thin Solid Films 518 (2010) 5745-5752.
54. J. Sleven, C. Görller-Walrand, K. Binnemans, Mater. Sci. Eng. C 18 (2001) 229-238.
55. T.V. Basova, B.A. Kolesov, A.G. Gürek, V. Ahsen, Thin Solid Films 385 (2001) 246-251.
56. K. Hatsusaka, K. Ohta, I. Yamamoto, H. Shirai, J. Mater. Chem. 11 (2001) 423-433.
57. J. Sleven,T. Cardinaels, C. Görller-Walrand, K. Binnemans, Arkivoc 4 (2003) 68-82.
58. J. Hoogboom, P.M. L. Garcia, M. B. J. Otten, J. A. A. W. Elemans, J. Sly, S. V. Lazarenko, T. Rasing, A. E. Rowan, R. J. M. Nolte, J. Am. Chem. Soc. 127 (2005) 11047-11052.
59. M.J. Cook, The Chemical Record 2 (2002) 225-236.
60. M. Durmuş, C. Lebrun, V. Ahsen, J. Porphyrins Phthalocyanine 8 (2004) 1175-1186.
61. C.A. Hunter, J. Sanders, J. Am. Chem. Soc. 112 (1990) 5525-5534.
62. Y. Suda, K. Shigehara, A. Yamada, H. Matsuda, S. Okada, A. Masaki, H. Nakanishi, Proc. SPIE-Int. SOC. Opt. Eng. 1560 (1991) 75-83.
63. D. Adam, P. Schuhmacher, J. Simmerer, L. Haussling, K. Siemensmeyer, K. H. Etzbach, H. Ringsdorf and D. Haarer, Nature 371 (1994) 141-143.
64. H. Eichhorn, D. Wöhrle, Liq. Cryst. 22 (1997) 643-653.
65. K. Ban, K. Nishizawa, K. Ohta, H. Shirai, J. Mater. Chem. 10 (2000) 1083-1090.
66. A.G. Gürek, Ö. Bekaroğlu, J. Chem. Soc. Dalton Trans. (1994) 1419-1423.

67. T.V. Basova, A.G. Gürek, V. Ahsen, Mater. Science and Engineering C 22 (2002) 99-104.
68. T. Basova, E. Kol'tsov, A.G. Gürek, D. Atilla, V. Ahsen, A.K. Hassan, Mater. Sci. Eng. C 28 (2008) 303-308.
69. C. Piechocki, J.C. Boulou, J. Simon, Mol. Cryst. Liq. Cryst. 149 (1987) 115-120.
70. D. Masurel, C. Sirlin, J. Simon, New J. Chem. 11 (1987) 455-456.
71. K. Ohta, L. Jacquemin, C. Sirlin, L. Bosio, J. Simon, New J. Chem. 12 (1988) 751-754.
72. D. Atilla, A.G. Gürek, T.V. Basova, V.G. Kiselev, A.K. Hassan, L.A. Sheludyakova, V. Ahsen, Dyes Pigments 88 (2011) 280-289.
73. S.Tuncel, H.A.J. Banimuslem, M. Durmuş, A.G. Gürek,V. Ahsen, T.V. Basova, A.K. Hassan, New J. Chem. 36 (2012) 1665-1672.
74. S. Tuncel, T.V. Basova, V.G. Kiselev, S.A. Gromilov, I.V. Jushina, M. Durmuş, A.G. Gürek, V. Ahsen, J. Mater. Res. 26 (2011) 2962-2973.
75. K. Ban, K. Nishizawa, K. Ohta, A.M. van de Craats, J.M. Warman, I. Yamamoto, H. Shirari, J. Mater. Chem. 11 (2001) 321-331.
76. A.G. Gürek, V. Ahsen, D. Luneau,J.Pecaut, Inorg. Chem. 40 (2001) 4793-4797.
77. A.G. Gürek, T. Basova, D. Luneau, C. Lebrun, E. Kol'tsov,A.K. Hassan, V. Ahsen, Inorg. Chem. 45 (2006) 1667-1676.
78. T. Basova, E. Kol'tsov, A.K. Hassan, A.K. Ray, A.G. Gürek, V. Ahsen, Mater. Chem. Phys. 96 (2006) 129-135.
79. T. Komatsu, K. Ohta, T. Watanabe, H. Ikemoto, T. Fujimoto, I. Yamamoto, J. Mater. Chem. 4 (1994) 537-540.
80. T. Basova, E. Kol'tsov, A.K. Hassan, A. Nabok, A. Ray, A.G. Gürek, V. Ahsen, J. Mater. Sci. Mater. Electron. 15 (2004) 623-628.
81. F. Maeda, K. Hatsusaka, K. Ohta, M. Kimura, J. Mater. Chem. 13 (2003) 243-251.
82. A.M. van de Craats, J.M. Warman, H. Hasebe, R. Naito, K. Ohta, J. Phys. Chem. B 101 (1997) 9224-9232.
83. P.G. Schoute, J.F. van der Pol, J.W. Zwikker, W. Drenth, S.J. Picken, Mol. Cryst. Liq. Cryst. 195 (1991) 291-305.
84. D. Lelievre, M.A. Petit, J. Simon, Liq. Cryst. 4 (1989) 707-710.
85. İ. Gürol, V. Ahsen, Ö. Bekaroğlu, J. Chem. Soc. Dalton Trans. 4 (1994) 497-500.
86. A.G. Gürek, V. Ahsen, F. Heinemann, P. Zugenmaier, Mol. Cryst. Liq. Cryst. 338 (2000) 75-97.
87. K. Ohta, S. Azumane, T. Watanahe, S. Tsukada. I. Yamamoto, Appl. Organomet. Chem. 10 (1996) 623-635.
88. A.G. Gürek,M. Durmuş, V. Ahsen, New J. Chem. 28 (2004) 693-699.

89. N.B. McKeown, I. Chambrier, M.J. Cook, J. Chem. Soc. Perkin Trans. 1 (1990) 1169-1177.
90. A.S. Cherodian, A.N. Davies, R.M. Richardson, M.J Cook, N.B. McKeown, A.J. Thomson, J. Feijoo, G. Ungar, K.J. Harrison, Mol. Cryst. Liq. Cryst. 196 (1991) 103-114.
91. H. Iino, J. Hanna, R.J. Bushby, B. Movaghar, B.J. Whitaker, M.J. Cook, Appl. Phys. Lett. 87 (2005) 132102.
92. D.J. Tate, R. Anémian, R.J. Bushby, S. Nanan, S.L. Warriner, B.J. Whitaker, Beilstein J. Org. Chem. 8 (2012) 120-128.
93. S. Sergeyev, E. Pouzet, O. Debever, J. Levin, J. Gierschner, J. Cornil, R. G. Aspe, Y.H. Geerts, J. Mater. Chem. 17 (2007) 1777-1784.
94. S. Sergeyev, O. Debever, E. Pouzet, Y. H. Geerts, J. Mater. Chem. 17 (2007) 3002-3007.
95. A. Hayer, V. de Halleux, A. Köhler, A. El-Garoughy, E. W. Meijer, J. Barbera, J. Tant, J. Levin, M. Lehmann, J. Gierschner, J. Cornil, Y. H. Geerts, J. Phys. Chem. B 110 (2006) 7653-7659.
96. W. Pisula, M. Kastler, B. El Hamaoui, M.-C. Garcia-Gutierrez, R. J.Davies, C. Riekel, K. Muellen, ChemPhysChem 8 (2007) 1025-1028.
97. S. Sergeyev, J. Levin, J.-Y. Balandier, E.Pouzet and Y. H. Geerts, Mendeleev Commun. 19 (2009) 185-186.
98. V. De Cupere, J. Tant, P. Viville, R. Lazzaroni, W. Osikowicz, W.R. Salaneck, Y.H. Geerts, Langmuir 22 (2006) 7798-7806.
99. T.V. Basova, M. Durmus, A.G. Gurek, V. Ahsen, A. Hassan, J. Phys. Chem. C 113 (2009) 19251-19257.
100. A. Calò, P. Stoliar, M. Cavallini, Y.H. Geerts, F. Biscarini, Rew. Sci. Instrum. 81 (2010) 033907.
101. M.P. de Jong, W. Osikowicz, S.L. Sorensen, S. Sergeyev, Y.H. Geerts, W.R. Salaneck, J. Phys. Chem. C 112 (2008) 15784-15790.
102. N.B. Chaure, C. Pal, S. Barard, T. Kreouzis, A.K. Ray, A.N. Cammidge, I. Chambrier, M. J. Cook, C. E. Murphy, M.G. Cain, J. Mater. Chem. 22 (2012) 19179-19189.
103. N. Chaure, T. Basova, M. Zahedi, A. Ray, A. Sharma, M. Durmuş, V. Ahsen J. Appl. Phys. 107 (2010) 114503.
104. T. Faris, T. Basova, N.B. Chaure, A.K. Sharma, M. Durmuş, V. Ahsen, A.K. Ray, EPL 106 (2014) 58002.
105. M. Wang, Y.-L. Yang, K. Deng, C. Wang, Chem. Phys. Lett. 439 (2007) 76-80.
106. T. Basova, C. Taşaltin, A.G. Gurek, M.A. Ebeoğlu, Z.Z. Öztürk, V. Ahsen, Sens. Actuators B, 96 (2003) 70-75.

107. T.V. Basova, M.Çamur, A.A. Esenpınar, S. Tuncel, A. Hassan, A. Alexeyev, H. Banimuslem, M. Durmuş, A.G. Gürek, V. Ahsen, Synth. Met. 162 (2012) 735-742.
108. E. Smela, L.J. Martinez-Miranda, J. Appl. Phys. 73 (1993) 3299-3304.
109. S. Paul, D. Paul, T. Basova, A. Ray, IET Nanobiotechnology 4 (2010) 1-9.
110. S. Wu, Polymer Interface and Adhesion. New York, Dekker, 1982.
111. J. Simmerer, B. Glüsen, W. Paulus, A. Kettner, P. Schuhmacher, D. Adam, K.-H. Etzbach, K. Siemensmeyer, J. H. Wendorff, H. Ringsdorf, D. Haarer, Adv. Mater. 8 (1996) 815-819.
112. G. Gbabode, N. Dumont, F. Quist, G. Schweicher, A. Moser, P. Viville, R. Lazzaroni, Y.H. Geerts, Adv. Mater. 24 (2012) 658-662.
113. K. Ukei, J. Phys. Soc. Jpn. 40 (1976) 140-143.
114. T. Basova, A.G. Gürek, D. Atilla, A. Hassan, V. Ahsen, Polyhedron 26 (2007) 5045-5052.
115. S. Dong, H. Tian, D. Song, Z. Yang, D. Yan, Y. Geng, F. Wang, Chem. Commun. 21 (2009) 3086-3088.
116. J. Cattle, P. Bao, J.P. Bramble, R.J. Bushby, S.D. Evans, J.E. Lydon, D.J. Tate, Adv. Funct. Mater. 23 (2013) 5997-6006.
117. P.O. Mouthuy, S. Melinte, Y.H. Geerts, B. Nysten, A.M. Jonas, Small 4 (2008) 728-732.
118. P.O. Mouthuy , S. Melinte, Y.H. Geerts, A.M. Jonas, Nano Lett. 7 (2007) 2627-2632.
119. J.P. Bramble, D.J. Tate, D.J. Revill, K.H. Sheikh, J. R. Henderson, F. Liu, X. Zeng, G. Ungar, R. J. Bushby, S.D. Evans, Adv. Funct. Mater. 20 (2010) 914-920.
120. M. Mas-Torrent, S. Masirek, P. Hadley, N. Crivillers, N.S. Oxtoby, P. Reuter, J. Veciana, C. Rovira, A. Tracz, Org. Electron. 9 (2008) 143-148.
121. M. Yoshio, T. Kagata, K. Hoshino, T. Mukai, H. Ohno, T. Kato, J. Am. Chem. Soc. 128 (2006) 5570-5577.
122. A. Tracz, T. Makowski, S. Masirek, W. Pisula, Y. Geerts, Nanotechnology 18 (2007) 485303.
123. D.V. Anokhin, M. Rosenthal, T. Makowski, A. Tracz, W. Bras, K. Kvashnina, D.A. Ivanov, Thin Solid Films 517 (2008) 982-985.
124. F. Latteyer, S. Savu, H. Peisert, T. Chassé, J. Raman Spectrosc. 43 (2012) 1227-1236.
125. Z. Belarbi, J. Phys. Chem. 94(1990) 7334-7336.
126. W.P. Hu, Y.Q. Liu, S.Q. Zhou, J. Tao, D.F. Xu, D.B. Zhu, Thin Solid Films 347 (1999) 299-301.
127. Y. Kitahama, Y. Kimura, K. Takazawa, Langmuir 22 (2006) 7600-7604.
128. J.-H. Lee, H.-S. Kim, B.D. Pate, S.-M. Choi, Physica B 385-386 (2006) 798-800.
129. J-H. Lee, S.-M. Choi, B.D. Pate, M.H. Chisholm, Y.-S. Han, J. Mater. Chem. 16 (2006) 2785-2791.

130. V. Duzhko, K.D. Singer, J. Phys. Chem. C 111 (2007) 27-31.
131. I. Dierking, Texture of Liquid Crystal, Wiley-VCH, Weinheim, Germany, 2003.
132. E. Venuti, R. G. Della Valle, I. Bilotti, A. Brillante, M. Cavallini, A. Calò, Y.H. Geerts, J. Phys. Chem. C 115 (2011) 12150–12157.
133. C. Deibel, D. Janssen, P. Heremans, V. De Cupere, Y. Geerts, M.L. Benkhedir, G.J. Adriaenssens, Organic Electronics 7 (2006) 495-499.
134. T. Basova, A. Hassan, M. Durmuş, A.G. Gürek, V. Ahsen, Synthetic Metals, 161 (2011) 1996-2000.
135. T. Basova, A.G. Gürek, V. Ahsen, A.K. Ray, Organic Electronics 8 (2007) 784-790.
136. K. Hatsusaka, M. Kimura, K. Otha, Bull. Chem. Soc. Jpn. 76 (2003) 781-787.
137. M. Ariyoshia, M. Sugibayashi-Kajitaa, A. Suzuki-Ichiharaa, T. Kato, T. Kamei, E. Itoh, K. Ohta, J. Porphyrins Phthalocyanines 16 (2012) 1114-1123.
138. M. Ichihara, M. Miida, B. Mohr, K. Ohta, J. Porphyrins Phthalocyanines 10 (2006) 1145-1155.
139. T. Kamei, T. Kato, E. Itoh, K. Ohta, J. Porphyrins Phthalocyanines 16 (2012) 1261-1275.
140. L. Tauchi, T. Nakagaki, M. Shimizu, E. Itoh, M. Yasutake, K. Ohta, J. Porphyrins Phthalocyanines 17 (2013) 1080-1093.
141. G. Schweicher, G. Gbabode, F. Quist, O. Debever, N. Dumont, S. Sergeyev, Y.H. Geerts, Chem. Mater. 21 (2009) 5867-5874.
142. J. Tant, Y.H. Geerts, M. Lehmann, V. De Cupere, G. Zucchi, B.W. Laursen, T. Bjornholm, V. Lemaur, V. Marcq, A. Burquel, E. Hennebicq, F. Gardebien, P. Viville, D. Beljonne, R. Lazzaroni, J. Cornil, J. Phys. Chem. B 110 (2006) 3449.
143. E. Charlet, P. Grelet, H. Bock, H. Saadaoui, L. Cisse, P. Destruel, N. Gheradi, I. Sequy, Appl. Phys. Lett. 92 (2008) 024107.
144. E. Grelet, H. Bock, Europhys. Lett. 73 (2006) 712-718.
145. E. Pouzet, V. De Cupere, C. Heintz, J.W. Andreasen, D.W. Breiby, M.M. Nielsen, P. Viville, R. Lazzaroni, G. Gbabode, Y.H. Geerts, J. Phys. Chem. C 113 (2009) 14398-14406.
146. U. Siemeling, C. Schirrmacher, U. Glebe, C. Bruhn, J.E. Baio, L. Árnadóttir, D. G. Castner, T. Weidner, Inorg. Chim. Acta 374 (2011) 302-312.
147. J. Hoogboom, P.M.L. Garcia, M.B.J. Otten, J.A.A.W. Elemans, J. Sly, S.V. Lazarenko, T. Rasing, A.E. Rowan, R.J.M. Nolte, J. Am. Chem. Soc. 127 (2005) 11047-11052.
148. J. Hoogboom, J.A.A.W Elemans, T. Rasing, A. E. Rowan, R.J.M. Nolte, Polym. Int. 56 (2007) 1186-1191.
149. C.F. van Nostrum, S.J. Picken, A.-J. Schouten, R.J.M. Nolte J. Am. Chem. Soc. 117 (1995) 9957-9965.

Figure captions

Figure 1. A schematic showing columns stacked on a regular hexagonal lattice, called Col_h; on a rectangular lattice, Col_r; an oblique lattice, Col_{ob}; etc.

Figure 2. Scheme of the homeotropic and planar(homogeneous) alignment of phthalocyanine films.

Figure 3. The structures of phthalocyanines bearing peripheral monoaza-crown ethers.

Figure 4. (a) - Optical texture of CuPc (**2**) observed at 130 ^{o}C (magnification 16x). Reproduced from Ref. [47] with kind permission of Pergamon. (b) - Optical texture of the CuPc (**5**) observed at 180 °C. The scale bar indicates 100 μm. Reproduced from Ref. [53] with kind permission of Elsevier S.A.

Figure 5. Phase transition temperature *vs.* number of carbon atoms in the alkoxy chain (n) for the $[(C_nO)_2PhO]_8PcCu$ (n=9-14) derivatives (**6a-f**). Reproduced from Ref. [56] with kind permission of Royal Society of Chemistry.

Figure 6. Optical textures of peripheral ((2,9(10),16(17),23(24)-positions)-tetra (13,17-dioxa-nonacosane -15-hydroxy)-substituted phthalocyanines observed at 25 °C (magnification × 25) (A (**10a**), B(**10b**), C(**10c**)). Reproduced from Ref. [60] with kind permission of World Scientific Publishing.

Figure 7. A mosaic texture observed under crossed polarizers (a) and X-ray diffraction pattern of octakis-hexylthiosubstituted Cu(II) phthalocyanine (**11b**) at room temperature. Reproduced from Ref. [68] with kind permission of Elsevier S.A.

Figure 8. The optical texture of PbPc-**13a** (A), observed at 160 °C and PbPc-**13b** (B) observed at room temperature. Reproduced from Refs. [72, 73] with kind permission of Pergamon and Royal Society of Chemistry.

Figure 9. Optical texture of (a) PbPc-**15**, (b) PbPc-**16**, and (c) PbPc-**18** complexes at room temperature Reproduced from Ref. [74] with kind permission of Materials Research Society; American Institute of Physics.

Figure 10. Bis[octakis(hexylthio)phthalocyaninato] Rare-Earth Metal(III) complexes(**19**-**22**).

Figure 11. The optical texture of $[(C_6S)_8Pc]_2Sm$ (**22**) at 140°C. Reproduced from Ref. [77] with kind permission of American Chemical Society.

Figure 12. Spherulite-like texture of compound **23**. Reproduced from Ref. [86] with kind permission of Taylor & Francis Group.

Figure 13. The optical texture of **24** observed at 250 °C (Magnification x25). Reproduced from Ref. [88] with kind permission of the Royal Society of Chemistry.

Figure 14. Optical micrographs taken with crossed polarisers at a magnification of × 20. (a) *n*-Octyl derivative **25** in the Col_h phase at 145 °C. (b) **25** in the Col_r phase at 100 °C. (c) Isooctyl derivative **26** in the Col_h phase at 170 °C. (d) **25** in the unknown (but probably Cr) phase at 120 °C. (e) Isoheptyl derivative **27** in the Col_h phase at 170 °C. (f) **27** in the C_r phase at 155 °C [92].

Figure 15. POM images of octakis -oligo(ethyleneoxy) substituted phthalocyanines (**28**) under parallel (A) and crossed (B) polarizers. Reproduced from Ref. [97] with kind permission of Elsevier S.A.

Figure 16. POM images under crossed polarizers of a **1b** film spin-coated on glass with a thickness of about 200 nm after annealing with a cooling rate of 0.1 °C/min. The white crosses indicate the center from which the columns develop. Reproduced from Ref. [98] with kind permission of American Chemical Society.

Figure 17. TMAFM height (50x50 μm^2) (A) and phase (200x200 nm^2) (B) images of **1b** film spin coated on a glass substrate after annealing. Reproduced from Ref. [98] with kind permission of American Chemical Society.

Figure 18. Tapping mode AFM images of a mesomorphic spin-coated film of **1b**. Small-scale tapping amplitude (B) image of the columnar structure. The arrows in (B) point at the layer and domain boundaries, which can be parallel or oblique to the column direction. Reproduced from Ref. [44] with kind permission of American Chemical Society.

Figure 19. POM images under crossed polarizers of the films of $PbPcR_8$ with R=-$S(CH_2)_{15}CH_3$ (**13b**) (A) and R=-$S(CH_2)_7CH_3$ (**13a**) (B) spun onto glass slides with a thickness of about 50 μm at 140 ^oC after cooling from isotropic melts with a cooling rate of 1 °C/min.

Figure 20. Cross-section of the liquid crystal aligned in polymer microchannels. Reproduced from Ref. [116] with kind permission of WILEY VCH VERLAG GMBH & CO.

Figure 21. Schematic representation of a Col_h phase aligned across the channels. Reproduced from Ref. [116] with kind permission of WILEY VCH VERLAG GMBH & CO.

Figure 22. A schematic showing the creation of enlongated droplets of discotic LC. The droplets are created by dewetting from adjacent hydrophobic stripes onto hydrophilic stripes. Reproduced from Ref. [119] with kind permission of WILEY VCH VERLAG GMBH & CO.

Figure 23. Schematic illustration showing the zone casting process and columnar orientation in zone-cast films. Reproduced from Ref. [123] with kind permission of Elsevier S.A.

Figure 24. An arrangement of columnar stacks perpendicular to the magnetic field on a substrate. Reproduced from Ref. [129] with kind permission of Elsevier B.V.

Figure 25. Optical (a) and polarizing optical microscopy (b) images with cross-polarizers of a homeotropically aligned film of **24** deposited between two quartz substrates; schematic illustration of the macroscopic alignment with respect to incident light (arrow) (c). Reproduced from Ref. [99] with kind permission of American Chemical Society.

Figure 26. SEM images of the sample ITO/MPc **24**/Al (middle image) and polarizing optical microscopy images with cross-polarizers of the film of **24** with parallel alignment deposited on ITO surface (left image) and a homeotropically aligned films deposited between ITO and metal electrode (right image). Schematic illustrations of the macroscopic alignments are also given. Reproduced from Ref. [134] with kind permission of Elsevier S.A.

Figure 27. Possible origin and mechanism of perfect homeotropic alignment of phthalocyanine derivatives. Reproduced from Ref. [137] with kind permission of World Scientific Publishing.

Figure 28. Molecular structure of (a): $(C_nO)_{16}$TcCu (**29**) and (b): $(C_nO)_{16}$TzCu (**30**).

Figure 29. Molecular structure of Pc-C60 dyads.

Figure 30. A schematic demonstrating utilizing of sacrificial layer to induce homeotropic alignment of LC phthalocyanine film.

Figure 31. Structure of pyridine-functionalized siloxane used as a command layer [147, 148].

Table 1. Structures of peripherally tetra-substituted phthalocyanines

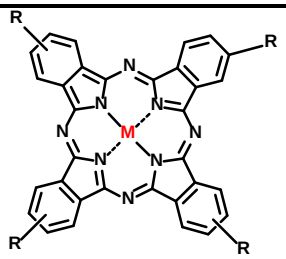

Compound	M	R
1a	2H	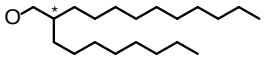
1b	2H	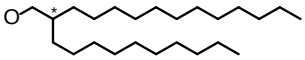
10a	2H	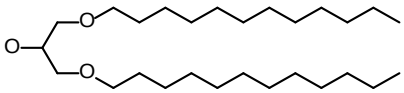
10b	Zn	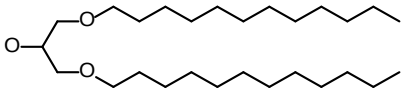
10c	Ni	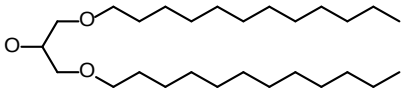
14	Pb	
15	Pb	
16	Pb	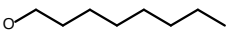
24	Ni	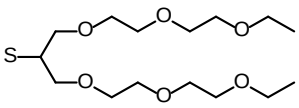
32	2H	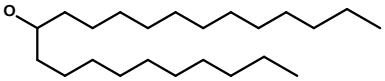

Table 2. Thermotropic properties of mesogens **1a** and **1b.** Reproduced from Ref. [43] with kind permission of American Chemical Society.

Compound	Phase behavior	Cell parameters (Å)	
H_2Pc-O-(12,8)$_4$	Col_r, 68 (0.05) Col_h	Col_r at 27^{o}C:	Col_h at 160^{o}C:
1a	226 (3.2) I	a = 46.7	a = 30.0
	I 225 (-3.2) Col_h	b = 29.8	
	68 (-0.08) Col_r		
H_2Pc-O-(14,10)$_4$	Col_r, 60 (0.05) Col_h	Col_r at 27^{o}C:	Col_h at 110^{o}C:
1b	180 (3.3) I	a = 52.1	a = 32.2
	I 174 (-3.2) Col_h	b = 32.5	
	57 (-0.05) Col_r		

Table 3. Phase transition temperatures and enthalpies for MPcs **3–5** as determined by DSC [53][a].

Compound	T(C→Col_h) / °C [ΔH / kJ mol^{-1}]	T(Col_h→C) / °C [ΔH / kJ mol^{-1}]
	Heating	**Cooling**
3, NiPc	60 [67.25]	42 [56.49]
4, ZnPc	77 [21.11] (only at the first cycle)	not observed
5, CuPc	73[60.30]	46 [69.55]

Heating and cooling rates: 10 °C, heating range: 25–300 °C.

[a] Phase nomenclature: Col_h=discotic hexagonal columnar mesophase, C=crystal.

Table 4. The structures of peripherally octa-substituted phthalocyanines

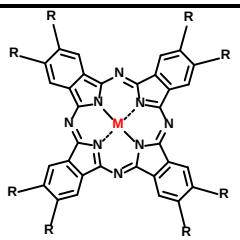

Compound	M	R
6a	Cu	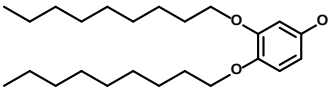
6b	Cu	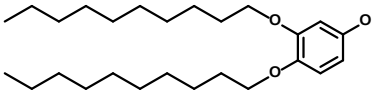
6c	Cu	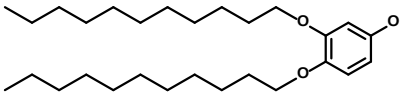
6d	Cu	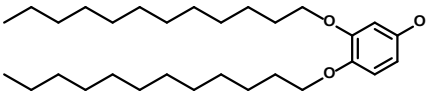
6e	Cu	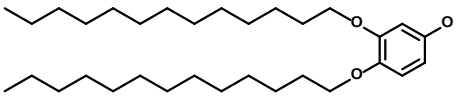
6f	Cu	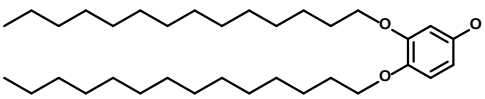
7a	Ni	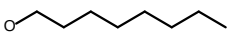
7b	Co	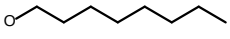
7c	Cu	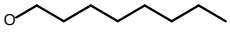
7d	Zn	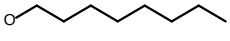
7e	2H	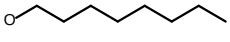
8a	Ni	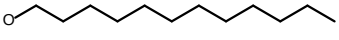
8b	Co	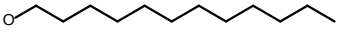
8c	Cu	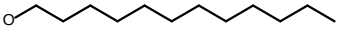
8d	Zn	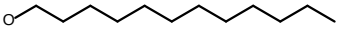
8e	2H	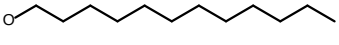

9a	Ni	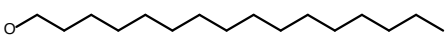
9b	Co	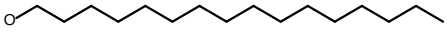
9c	Cu	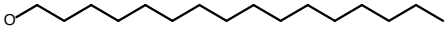
9d	Zn	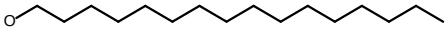
9e	2H	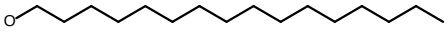
11a	Ni	
11b	Cu	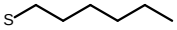
12a	Ni	
12b	Cu	
13a	Pb	
13b	Pb	
23	Ni	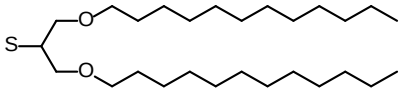
28	2H	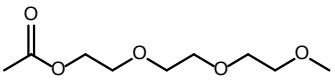
31	2H	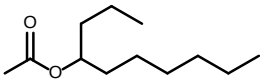

Table 5. Phase transition[a] temperatures (°C) and, in parentheses, enthalpy changes ΔH (in $kJ.mol^{-1}$) determined by DSC (heating and cooling rates are 10 $°C.min^{-1}$) for compounds **10a-c.** Reproduced from Ref. [60] with kind permission of World Scientific Publishing.

Compound	Heating		Cooling	
	$C \rightarrow Col_h \rightarrow I$		$I \rightarrow Col_h \rightarrow C$	
10a	14.2(90.35)	56.1(2.44)	38.4(2.31)	3.0(90.50)
10b	14.4(91.98)	116.9(6.26)	112.2(6.19)	7.5(91.89)
10c	11.5(84.21)	122.9(1.82)	114.0(1.96)	2.7(83.78)

[a] C: solid phase, Colh: hexagonally ordered discotic colomnar mesophase, I: isotropic phase

Table 6. X-ray diffraction data of the compound **10a-c** at room temperature. Reproduced from Ref. [60] with kind permission of World Scientific Publishing.

Compound	Spacing(Å)		Ratio	Miller indices	Lattice constant
	$d_{observed}$	$d_{calculated}$			
10a	30.25	30.05	1	100	
	17.54	17.35	√3	110	
	15.03	15.02	√4	200	
	11.59	11.35	√7	210	a=34.69 Å
	9.99	10.01	√9	300	
	8.80	8.68	√12	220	
	8.02	8.33	√13	310	
	4.84				
	3.75				
10b	32.36	32.36	1	100	
	18.50	18.68	√3	110	
	15.94	16.18	√4	200	
	12.02	12.23	√7	210	a=37.36 Å
	10.56	10.78	√9	300	
	9.15	9.34	√12	220	
	8.77	8.97	√13	310	
	4.85				
	3.35				
10c	30.25	30.25	1	100	
	17.34	17.46	√3	110	
	14.99	15.12	√4	200	
	11.36	11.43	√7	210	a=34.93 Å
	10.00	10.08	√9	300	

8.82	8.73	√12	220
7.99	8.38	√13	310
4.58			
3.49			

Table 7. Phase transition temperatures and enthalpy changes for the octa-hexyl or dodecyl-thiosubstituted Ni (II) (**11a,12a**) and Cu(II) (**11b**) phthalocyanines determined by DSC (heating and cooling rates are 10 °C min^{-1}, heating range is from −20 to 300 °C). Reproduced from Refs. [67, 68] with kind permission of Elsevier S.A.

Compound	Phase $\xrightarrow{(^{o}C)[\ H(kj\ mol^{-1}]}$ Phase
11a	$C \underset{}{\overset{36\ [92]}{\rightleftharpoons}} Col_h \xrightarrow{ca.\ 300} dec.$
12a	$C \underset{}{\overset{20\ [85]}{\rightleftharpoons}} Col_h \xrightarrow{ca.\ 275} dec.$
11b	$C \underset{-1\ [12.11]}{\overset{8\ [21.73]}{\rightleftharpoons}} Col_h \xrightarrow{ca.\ 300} dec.$

C is crystalline solid, Col_h is mesophase.

Table 8. Phase transition temperatures (corresponding enthalpy changes in parentheses) for the compounds **13a,b** and **14** determined by DSC. Heating and cooling rates: 10 °C, heating range: -25-250 °C. Phase nomenclature: C - crystal, Col_h - discotic hexagonal columnar mesophase, I - isotropic phase. Reproduced from Refs. [72, 73] with kindly permission of Pergamon and Royal Society of Chemisty.

Compound	Phase $\xrightarrow{(^oC)[\ H(kj\ mol^{-1}]}$ Phase
13a	$C \underset{-3.2\ [5.92]}{\overset{6.7\ [1.95]}{\rightleftharpoons}} Col_h \underset{222.9\ [2.42]}{\overset{240.0\ [1.44]}{\rightleftharpoons}} I$
13b	$C \underset{22.8\ [104.97]}{\overset{31.2\ [108.33]}{\rightleftharpoons}} Col_h \underset{184.7\ [3.65]}{\overset{204.5\ [7.43]}{\rightleftharpoons}} I$
14	$C \underset{56.7\ [23.7]}{\overset{65.1\ [24.9]}{\rightleftharpoons}} Col_h \underset{156.3\ [7.0]}{\overset{185.1\ [6.3]}{\rightleftharpoons}} I$

Table 9. The structures of non-peripherally tetra-substituted phthalocyanines

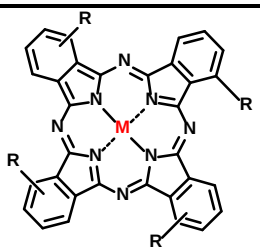

Compound	M	R
17	Pb	
18	Pb	

Table 10. Phase transition temperatures (°C) and enthalpy changes ΔH (in parentheses, kJ/mol) of PbPc complexes (**15-18**) obtained by differential scanning calorimetry (heating and cooling rates were 10 °C/min). Reproduced from Ref. [74] with kind permission of Materials Research Society, American Institute of Physics.

	Phase transition	
	First heating/cooling cycle	Second heating/cooling cycle
15	$Cr \xrightarrow{121\ [6.4]} Col_h \underset{216\ [10.4]}{\overset{232\ (7.0)}{\rightleftharpoons}} I$	$Col_h \underset{177\ [5.1]}{\overset{232\ [2.8]}{\rightleftharpoons}} I$
16	$Cr \xrightarrow{138\ [4.3]} Col_h \underset{156\ [6.7]}{\overset{188\ [11.8]}{\rightleftharpoons}} I$	$Col_h \underset{149\ [5.9]}{\overset{181\ [7.5]}{\rightleftharpoons}} I$
17	$A \underset{43\ [4.3]}{\overset{63\ [15.3]}{\rightleftharpoons}} I$	$A \underset{51\ [2.9]}{\overset{52\ [5.1]}{\rightleftharpoons}} I$
18	$Cr_1 \xrightarrow{69\ [3.8]} Cr_2 \xrightarrow{123\ [8.1]} Col_h \underset{110\ [21.7]}{\overset{141\ [19.3]}{\rightleftharpoons}} I$	$Col_t \underset{110\ [21.6]}{\overset{140\ [23.6]}{\rightleftharpoons}} I$

Phase nomenclature: Col_h, discotic hexagonal columnar; Col_t, discotic tetragonal columnar; I, isotropic phase; Cr, Cr_1, and Cr_2, crystal phases; and A, amorphous phase.

Table 11. Phase-Transition Temperature and Enthalpy Change Data for derivatives **19-22**[a]. Reproduced from Ref. [77, 78] American Chemical Society and Elsevier S.A.

Complex	Phase $\xrightarrow{(^{o}C)[\Delta H(kJ\ mol^{-1}]}$ Phase
19 Lu(PcR_8)$_2$	$K_{1V} \xrightarrow{102\ [59.55]} K_{2V} \xrightarrow{120\ [61.85]} Col_h \underset{232\ [-8.30]}{\overset{242\ [9.60]}{\rightleftharpoons}} IL$; $K_3 \underset{92\ [43.08]}{\rightleftharpoons} Col_h$
20 Gd(PcR_8)$_2$	$K \underset{81\ [29.86]}{\overset{52\ [22.75]}{\rightleftharpoons}} Col_h \underset{265\ [10.98]}{\overset{258\ [7.18]}{\rightleftharpoons}} IL$
21 Dy(PcR_8)$_2$	$K \underset{82\ [25.12]}{\overset{55\ [15.53]}{\rightleftharpoons}} Col_h \underset{263\ [10.54]}{\overset{250\ [8.19]}{\rightleftharpoons}} IL$
22 Sm(PcR_8)$_2$	$K \underset{81\ [28.38]}{\overset{60\ [16.92]}{\rightleftharpoons}} Col_h \underset{248\ [8.74]}{\overset{240\ [6.64]}{\rightleftharpoons}} IL$

[a] Phase nomenclature: K= crystal: Col_h: discotic hexagonal-columnar phase: IL= isotropic liquid

Table 12. X-ray powder diffraction data of the compound **23**. Reproduced Ref. [86] with kindly permission of Taylor & Francis Group.

d-spacing [Å]	*hkl*	Two dimensional rectangular cell dimensions[Å]
35.7 s[a]	110	
28.1 s	200	a= 56.2
17.8 w	220	b= 46.2
14.3 w	320	
12.0 w	420	
8.9 w	440	
4.8 md		
4.2 md		

[a] s: sharp; m:middle; w:weak; d:diffuse

Table 13. Phase transition temperatures and enthalpies for the tetra-substituted Ni(II) phthalocyanine derivative(**24**) as determined by DSC[a]. Reproduced Ref. [88] with kindly permission of Royal Society of Chemistry.

Compound	$T(Col_h \rightarrow I)$ / °C [ΔH / kJ mol^{-1}]	$T(I \rightarrow Col_h)$ / °C [ΔH / kJ mol^{-1}]
	Heating	**Cooling**
24	230.5 [0.906]	220.0 [0.614]

[a]Heating and cooling rates: 10 °C min^{-1}, heating range: 10–300 °C.

Table 14. X-Ray diffraction data of the tetra-substituted Ni(II) phthalocyanine derivative (**24**). Reproduced from Ref. [88] with kind permission of the Royal Society of Chemisty.

Compound	**Observed spacing / Å**	**Theoretical spacing / Å**	**Lattice constant / Å**	**Ratio**	**Miller indices**
24	22.76	22.76		1	(100)
	13.02	13.14		√3	(110)
	11.40	11.38	a = 26.28 Col_{hd} [a]	√4	(200)
	8.71	8.6		√7	(210)
	4.35	-			
	3.61	-			

Table 15. Structures of non-peripherally octa-substituted phthalocyanines

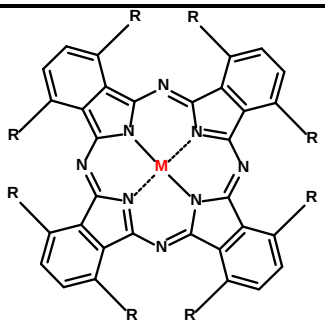

Compound	M	R
25	2H	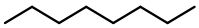
26	2H	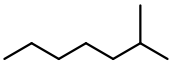
27	2H	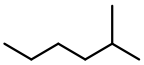

Table 16. Phase behaviour of the phthalocyanines(**25-27)** determined by DSC (second heating and first cooling cycle; heating/cooling rate of 10 °C min^{-1}) [92].

Compound	**Alkyl chain**	**Phase behaviour** °C (ΔH, $J \cdot g^{-1}$)
25	$-(CH_2)_6CH_3$	Cr 85 (10) Col_r 101 (0.05) Col_h 152 I 150 Col_h 96 Col_r 75 Cr
26	$-(CH_2)_5CH(CH_3)_2$	Cr_1 112 (15) Cr_2 (?)124 (9) Col_h 170 (11) I 162 (−11) Col_h 105 (−9) Cr_2 (?) 20 (−9) Cr_1
27	$-(CH_2)_4CH(CH_3)_2$	C_r 169 (14) Col_h 189 (35) I 169 (−17) Col_h161 (−14) C_{r1} 140 (−11) C_r

Table 17. Contact angles with water and hexadecane of the substrates. Reproduced from Ref. [98] with kind permission of American Chemical Society.

Substrate	Contact angle of water	Contact angle of hexadecane
glass	15±1°	7±2°
poly(isobutylene)	87±1°	-
ITO	66±1°	6±2°
gold	54±4°	9±3°
PEDOT:PSS	19±4°	12±2°
Fluorinated rubber (FKM); $[(CH_2\text{-}CF_2)0.6\text{-}(CF_2\text{-}CF(CF_3))0.4]_n$	81±4°	31±3°
[6,6]-Phenyl-C_{61}-butyric acid methyl ester (PCBM)	78±6°	5±1°
Si (with native SiO_2 layer)	65±3°	6±2°

Table 18. Results of attempts to align DLCs between 2.5 μm high SU8 barriers in channels which were 2 μm, 5 μm or 10 μm wide on a silicon substrate. In each case the experiment was conducted in exactly the same way and the sample was cooled from the isotropic phase at a rate of 0.1 ^{o}C/min. Reproduced from Ref. [116] with kind permission of WILEY VCH VERLAG GMBH & CO.

LC phthalocyanine	10 μm	5 μm	2 μm
H_2Pc **25**	NO	YES	YES
H_2Pc **26**	NO	NO	NO
H_2Pc **27**	NO	YES	YES

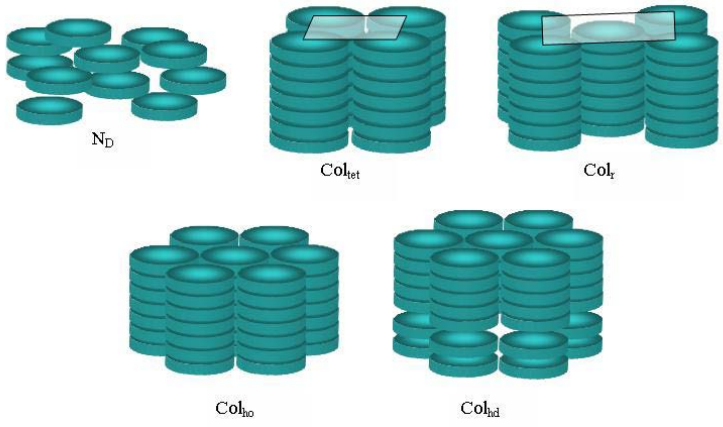

Figure 1. A schematic showing columns stacked on a regular hexagonal lattice, called Col_h; on a rectangular lattice, Col_r; an oblique lattice, Col_{ob}; etc.

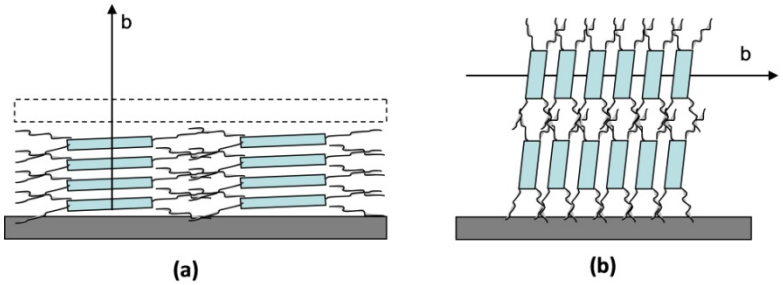

Figure 2. Scheme of the homeotropic and planar(homogeneous) alignment of phthalocyanine films.

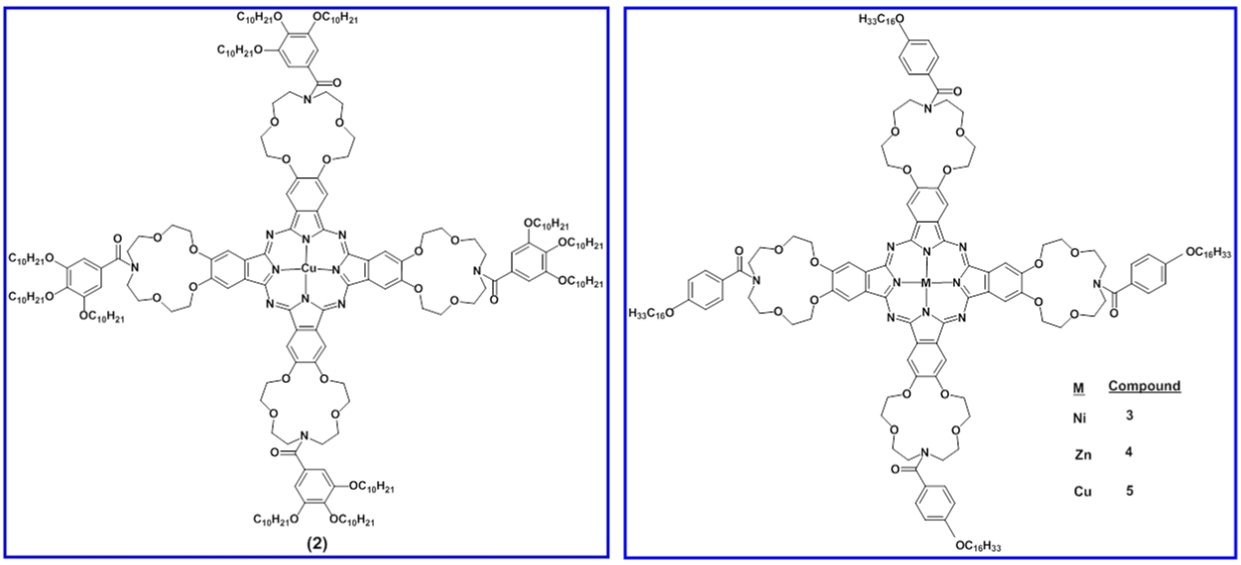

Figure 3. The structures of phthalocyanines bearing peripheral monoaza-crown ethers.

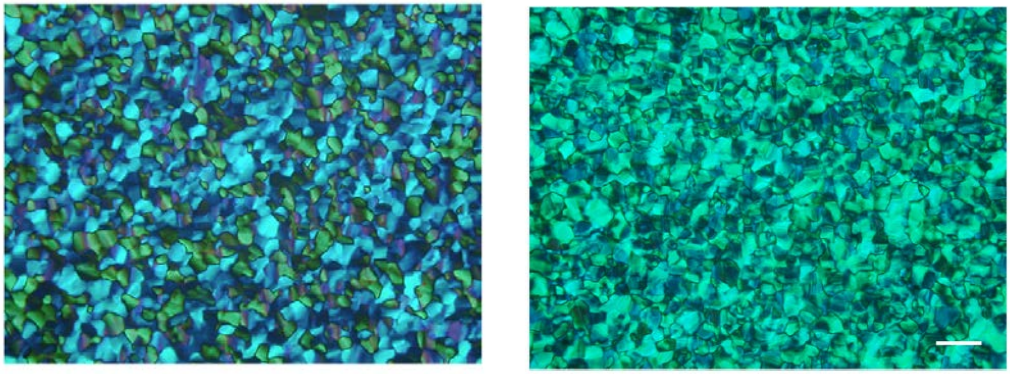

Figure 4. (a) - Optical texture of CuPc (**2**) observed at 130 ^{o}C (magnification 16x). Reproduced from Ref. [47] with kind permission of Pergamon. (b) - Optical texture of the CuPc (**5**) observed at 180 °C. The scale bar indicates 100 μm. Reproduced from Ref. [53] with kind permission of Elsevier S.A.

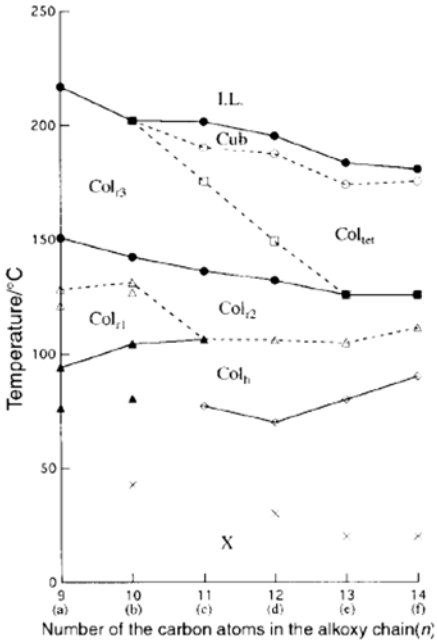

Figure 5. Phase transition temperature *vs.* number of carbon atoms in the alkoxy chain (n) for the $[(C_nO)_2PhO]_8PcCu$ (n=9-14) derivatives (**6a-f**). Reproduced from Ref. [56] with kind permission of Royal Society of Chemistry.

Figure 6. Optical textures of peripheral ((2,9(10),16(17),23(24)-positions)-tetra (13,17-dioxa-nonacosane -15-hydroxy)-substituted phthalocyanines observed at 25 °C (magnification × 25) (A (**10a**), B(**10b**), C(**10c**)). Reproduced from Ref. [60] with kind permission of World Scientific Publishing.

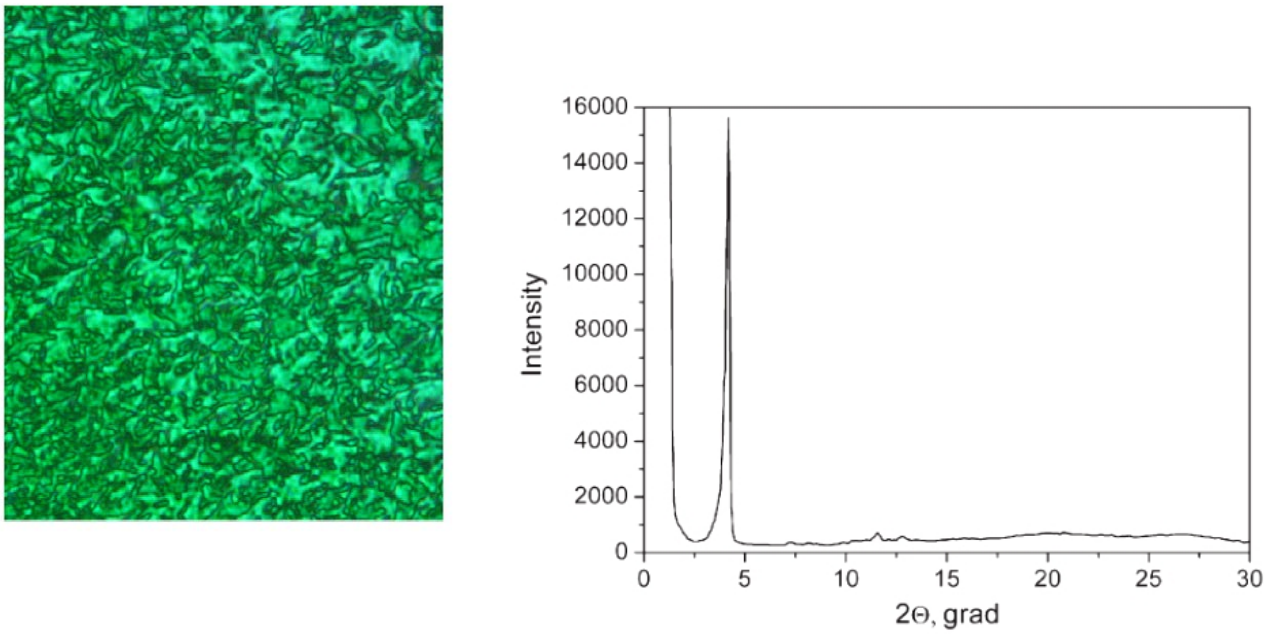

Figure 7. A mosaic texture observed under crossed polarizers (a) and X-ray diffraction pattern of octakis-hexylthiosubstituted Cu(II) phthalocyanine (**11b**) at room temperature. Reproduced from Ref. [68] with kind permission of Elsevier S.A.

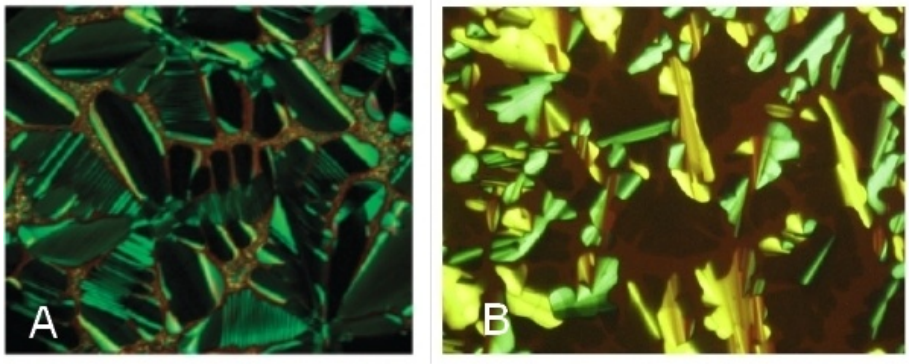

Figure 8. The optical texture of PbPc-**13a** (A), observed at 160 °C and PbPc-**13b** (B) observed at room temperature. Reproduced from Refs. [72, 73] with kind permission of Pergamon and Royal Society of Chemistry.

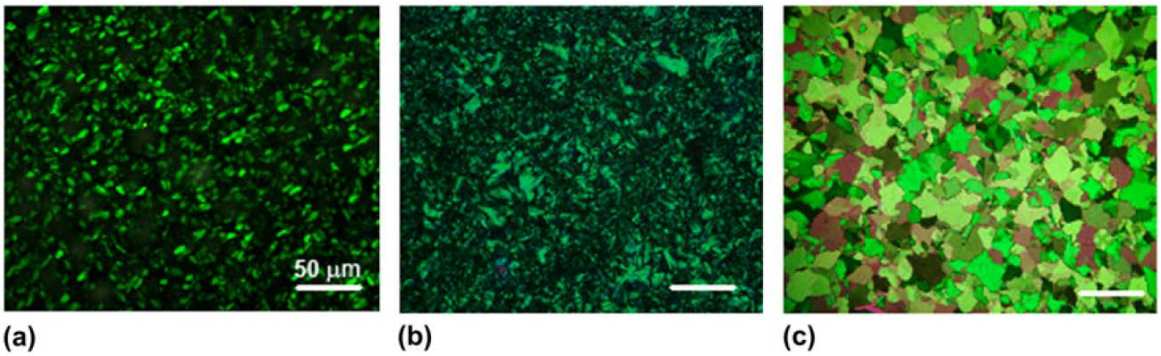

Figure 9. Optical texture of (a) PbPc-**15**, (b) PbPc-**16**, and (c) PbPc-**18** complexes at room temperature Reproduced from Ref. [74] with kind permission of Materials Research Society; American Institute of Physics.

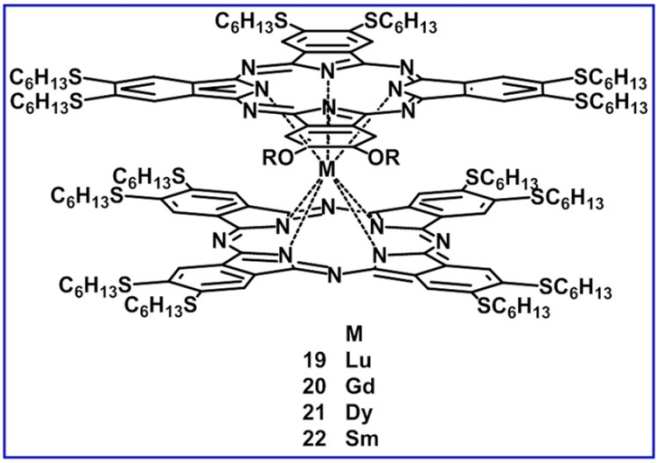

Figure 10. Bis[octakis(hexylthio)phthalocyaninato] Rare-Earth Metal(III) complexes(**19-22**).

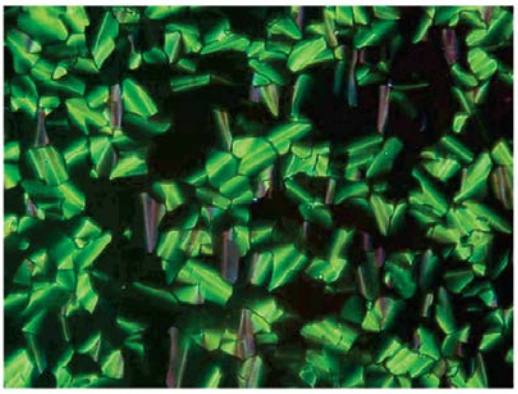

Figure 11. The optical texture of $[(C_6S)_8Pc]_2Sm$ (**22**) at 140°C. Reproduced from Ref. [77] with kind permission of American Chemical Society.

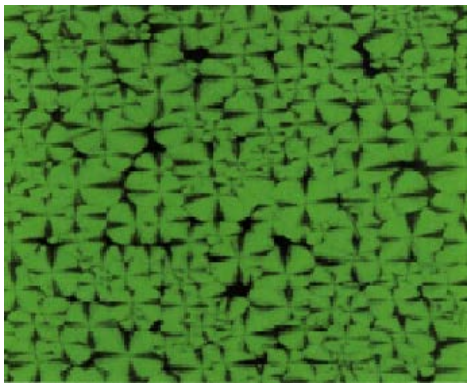

Figure 12. Spherulite-like texture of compound **23**. Reproduced from Ref. [86] with kind permission of Taylor & Francis Group.

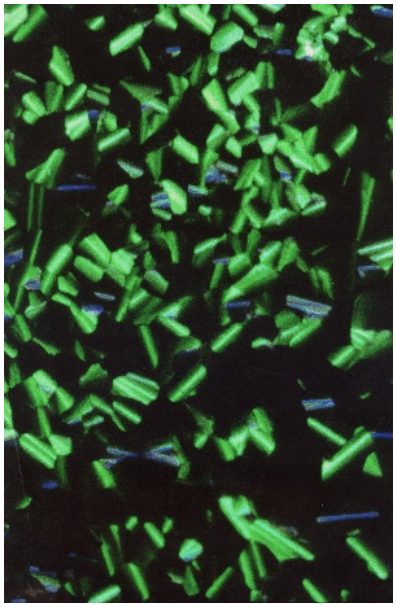

Figure 13. The optical texture of **24** observed at 250 °C (Magnification x25). Reproduced from Ref. [88] with kind permission of the Royal Society of Chemistry.

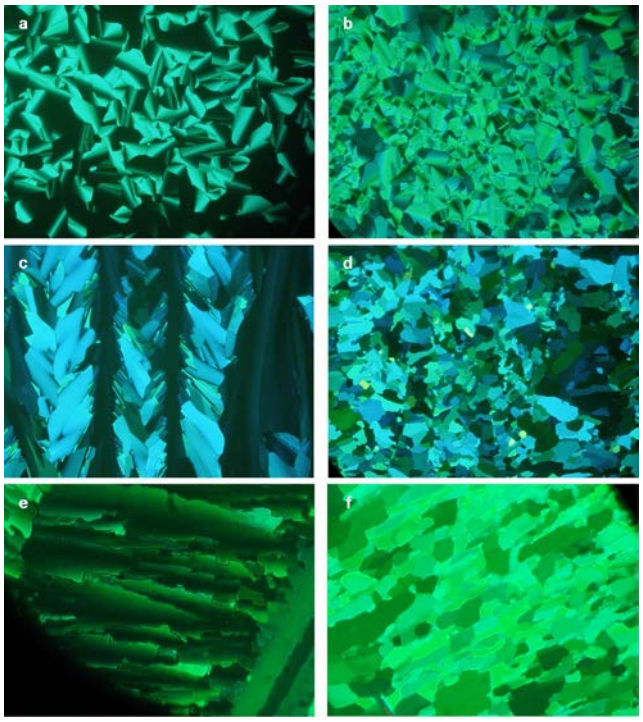

Figure 14. Optical micrographs taken with crossed polarisers at a magnification of × 20. (a) *n*-Octyl derivative **25** in the Col_h phase at 145 °C. (b) **25** in the Col_r phase at 100 °C. (c) Isooctyl derivative **26** in the Col_h phase at 170 °C. (d) **25** in the unknown (but probably Cr) phase at 120 °C. (e) Isoheptyl derivative **27** in the Col_h phase at 170 °C. (f) **27** in the C_r phase at 155 °C [92].

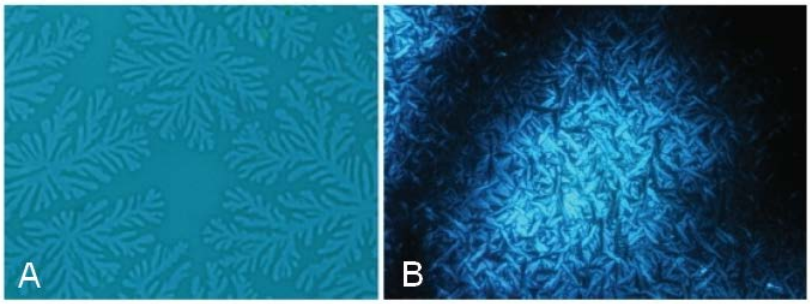

Figure 15. POM images of octakis -oligo(ethyleneoxy) substituted phthalocyanines (**28**) under parallel (A) and crossed (B) polarizers. Reproduced from Ref. [97] with kind permission of Elsevier S.A.

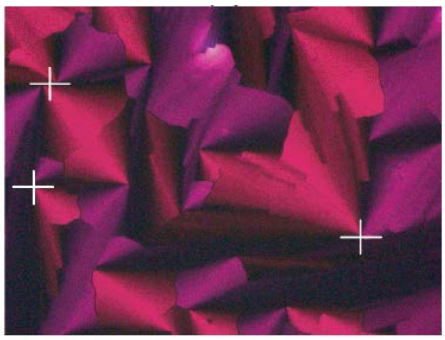

Figure 16. POM images under crossed polarizers of a **1b** film spin-coated on glass with a thickness of about 200 nm after annealing with a cooling rate of 0.1 °C/min. The white crosses indicate the center from which the columns develop. Reproduced from Ref. [98] with kind permission of American Chemical Society.

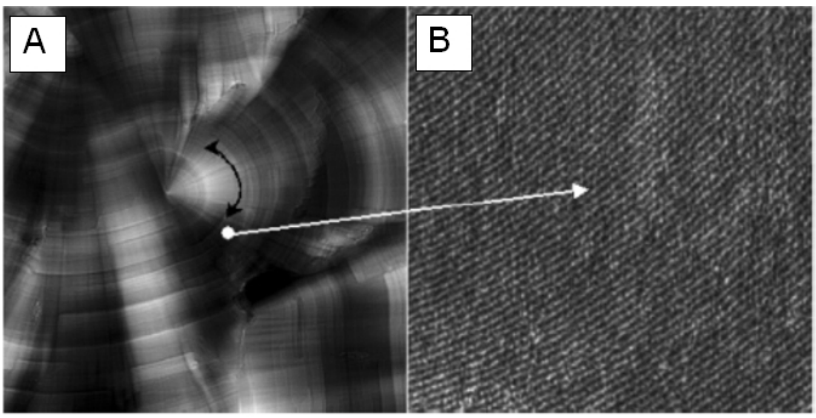

Figure 17. TMAFM height (50x50 μm^2) (A) and phase (200x200 nm^2) (B) images of **1b** film spin coated on a glass substrate after annealing. Reproduced from Ref. [98] with kind permission of American Chemical Society.

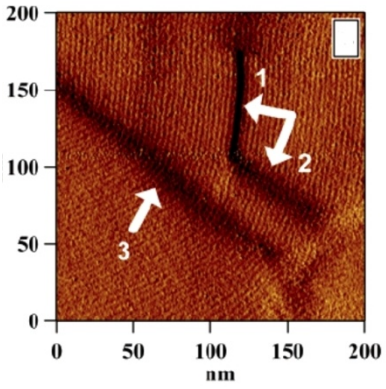

Figure 18. Tapping mode AFM images of a mesomorphic spin-coated film of **1b**. Small-scale tapping amplitude (B) image of the columnar structure. The arrows in (B) point at the layer and domain boundaries, which can be parallel or oblique to the column direction. Reproduced from Ref. [44] with kind permission of American Chemical Society.

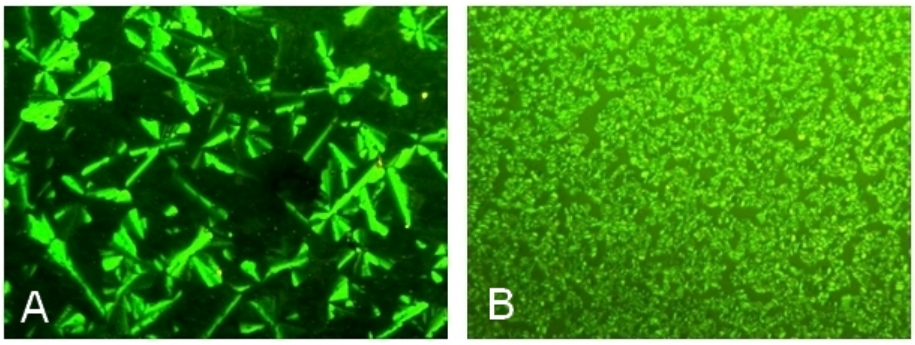

Figure 19. POM images under crossed polarizers of the films of $PbPcR_8$ with R=-$S(CH_2)_{15}CH_3$ (**13b**) (A) and R=-$S(CH_2)_7CH_3$ (**13a**) (B) spun onto glass slides with a thickness of about 50 μm at 140 ^oC after cooling from isotropic melts with a cooling rate of 1 °C/min.

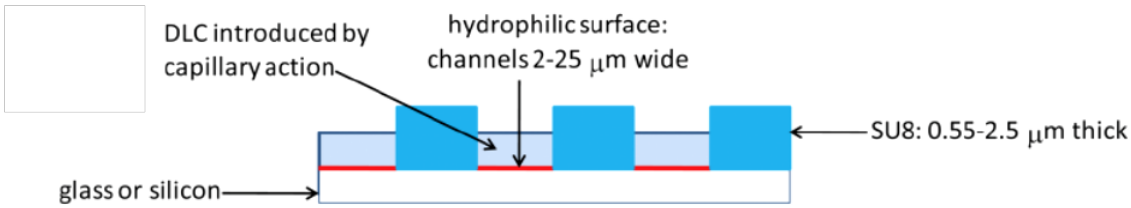

Figure 20. Cross-section of the liquid crystal aligned in polymer microchannels. Reproduced from Ref. [116] with kind permission of WILEY VCH VERLAG GMBH & CO.

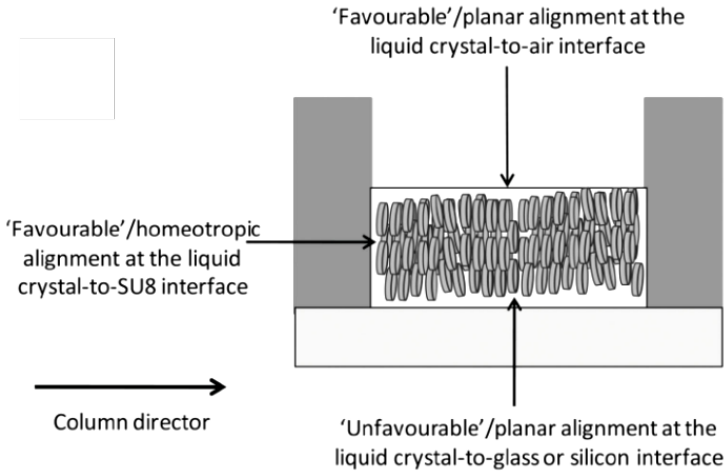

Figure 21. Schematic representation of a Col_h phase aligned across the channels. Reproduced from Ref. [116] with kind permission of WILEY VCH VERLAG GMBH & CO.

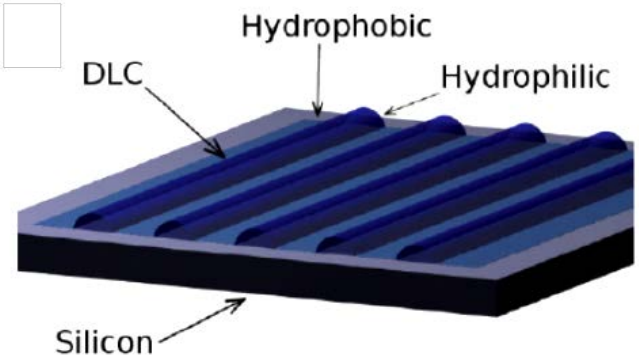

Figure 22. A schematic showing the creation of enlongated droplets of discotic LC. The droplets are created by dewetting from adjacent hydrophobic stripes onto hydrophilic stripes. Reproduced from Ref. [119] with kind permission of WILEY VCH VERLAG GMBH & CO.

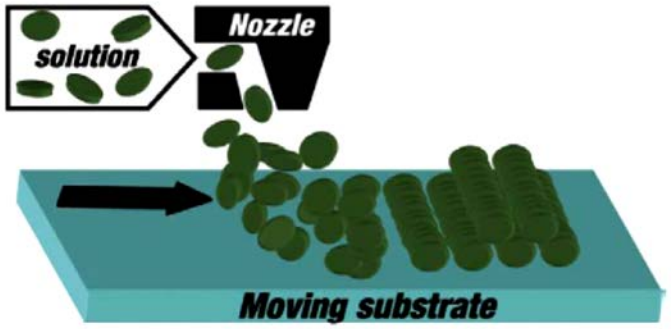

Figure 23. Schematic illustration showing the zone casting process and columnar orientation in zone-cast films. Reproduced from Ref. [123] with kind permission of Elsevier S.A.

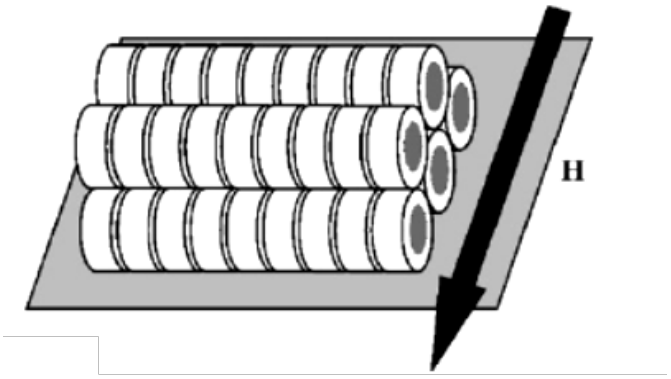

Figure 24. An arrangement of columnar stacks perpendicular to the magnetic field on a substrate. Reproduced from Ref. [129] with kind permission of Elsevier B.V.

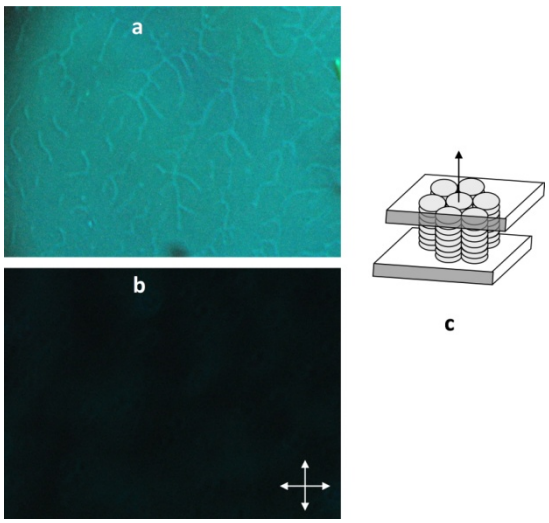

Figure 25. Optical (a) and polarizing optical microscopy (b) images with cross-polarizers of a homeotropically aligned film of **24** deposited between two quartz substrates; schematic illustration of the macroscopic alignment with respect to incident light (arrow) (c). Reproduced from Ref. [99] with kind permission of American Chemical Society.

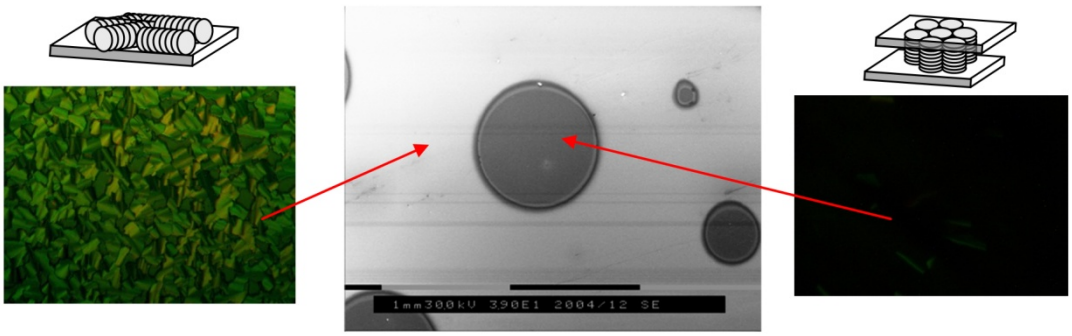

Figure 26. SEM images of the sample ITO/MPc **24**/Al (middle image) and polarizing optical microscopy images with cross-polarizers of the film of **24** with parallel alignment deposited on ITO surface (left image) and a homeotropically aligned films deposited between ITO and metal electrode (right image). Schematic illustrations of the macroscopic alignments are also given. Reproduced from Ref. [134] with kind permission of Elsevier S.A.

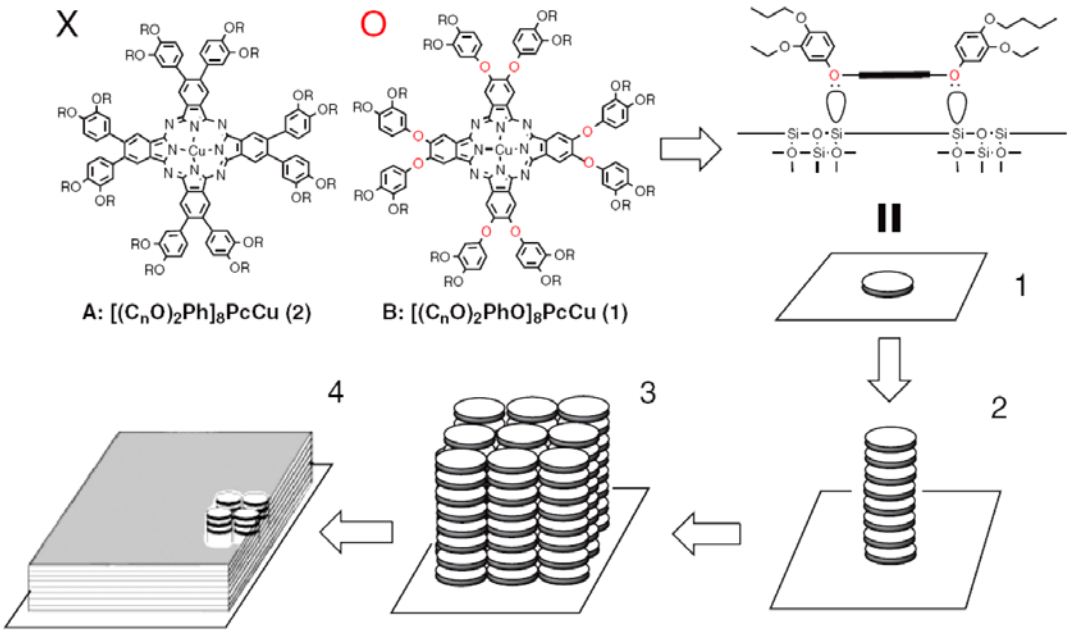

Figure 27. Possible origin and mechanism of perfect homeotropic alignment of phthalocyanine derivatives. Reproduced from Ref. [137] with kind permission of World Scientific Publishing.

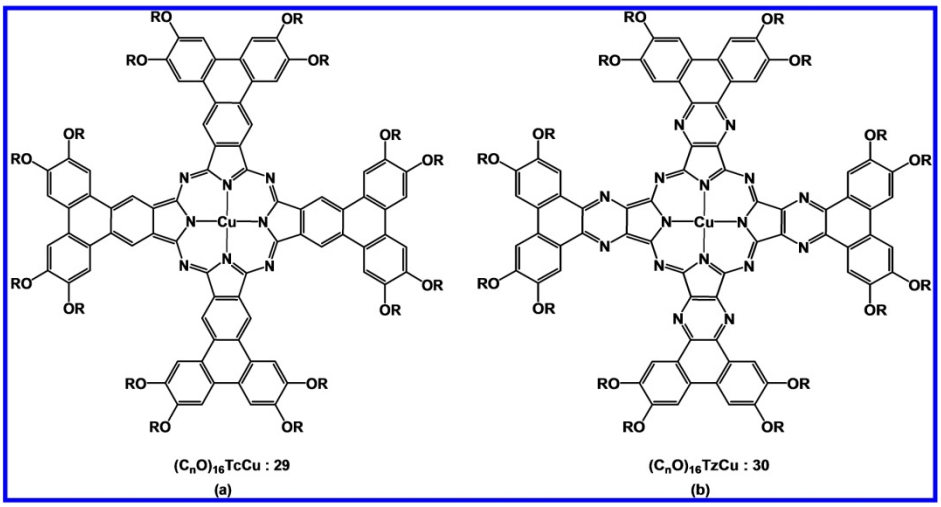

Figure 28. Molecular structure of (a): $(C_nO)_{16}$TcCu (**29**) and (b): $(C_nO)_{16}$TzCu (**30**).

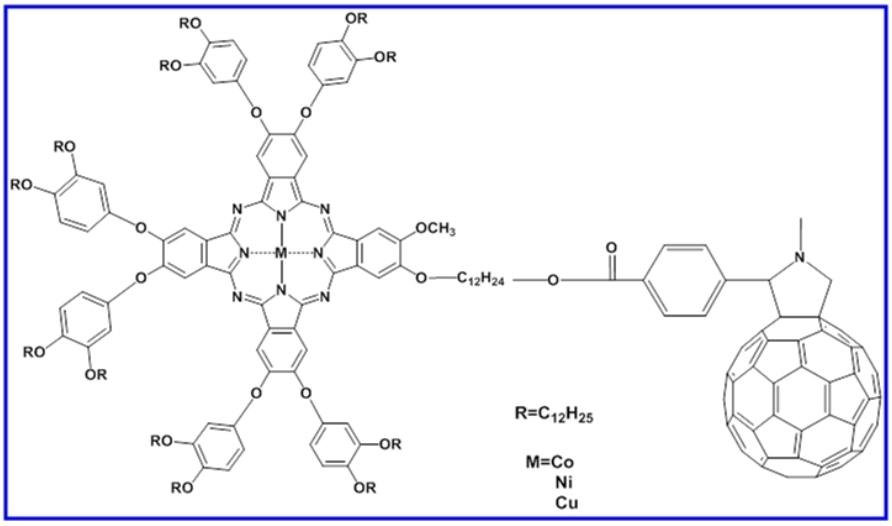

Figure 29. Molecular structure of Pc-C60 dyads.

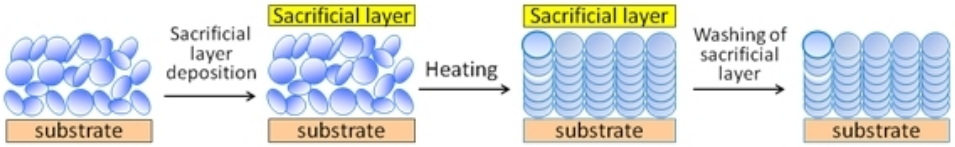

Figure 30. A schematic demonstrating utilizing of sacrificial layer to induce homeotropic alignment of LC phthalocyanine film.

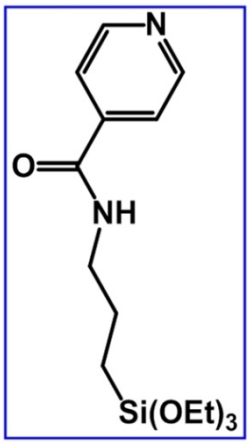

Figure 31. Structure of pyridine-functionalized siloxane used as a command layer [147, 148].